Wood Laminated Composite Poles

Cheng Piao

Louisiana Forest Product Lab

School of Renewable Natural Resources

Louisiana State University

Utility Poles

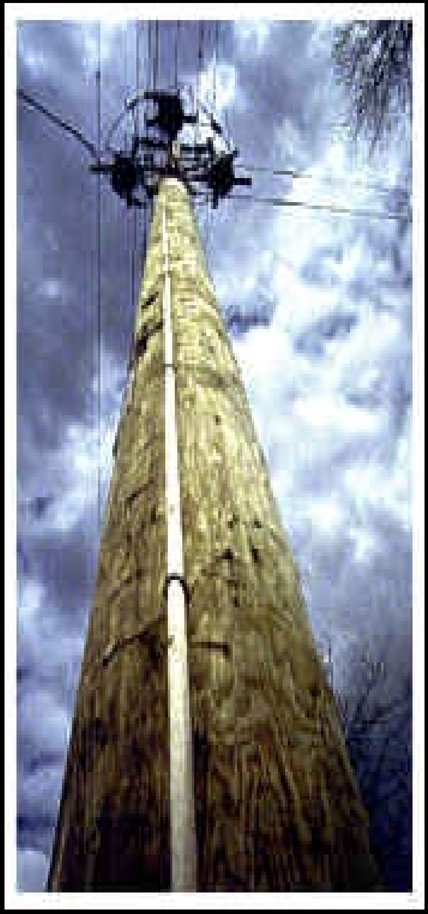

Wood Utility Pole Processing

Why Wood Utility Poles

- Produced from a renewable natural resource
- A cost-effective choice
- Easily climbed
- Easily machined

Species of Wood Utility Poles

- Wood utility poles for electrical distribution and telecommunications are manufactured from Red Pine, Jack Pine, Yellow Pine, Lodgepole Pine, Fir and Cedar, in accordance with CSA O15, ANSI 05 and many other international standards

Wood Laminated Composite Poles

- Hollow poles that have polygonal shapes
- Composed of trapezoid wood strips
- Bonded with synthetic resin

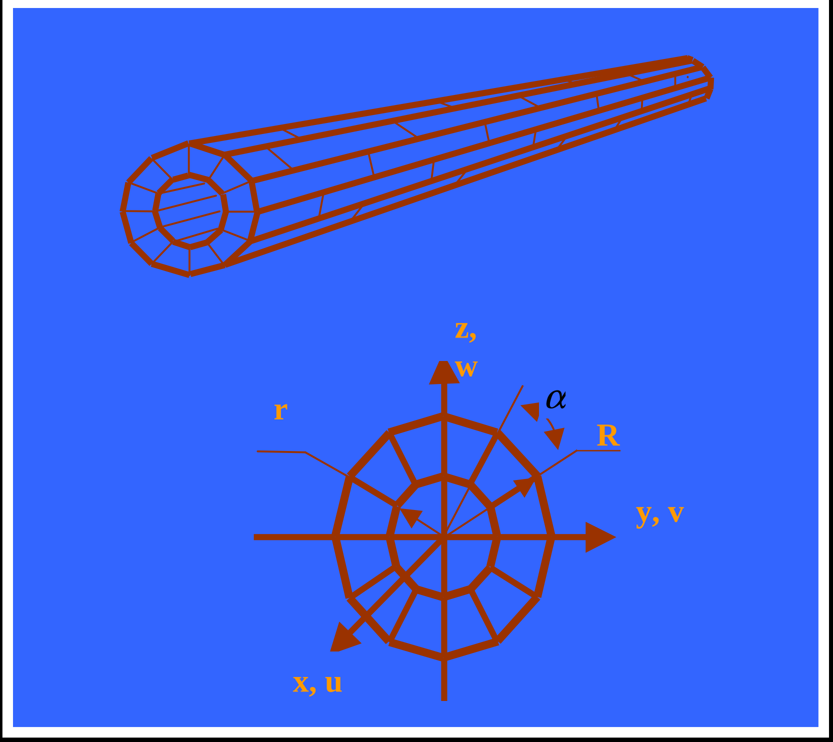

Why Wood Composite Poles

- Sufficient strength
- More cost-effective
- Light weight
- Freedom in sizes and shapes
- Environment considerations

Objectives

- Properties of wood composite poles
- Theoretical model development
- Finite element model development

Contents

- Experimental Study
- Theoretical Analysis
- Finite Element Analysis

Experimental Study

Components of Composite Poles

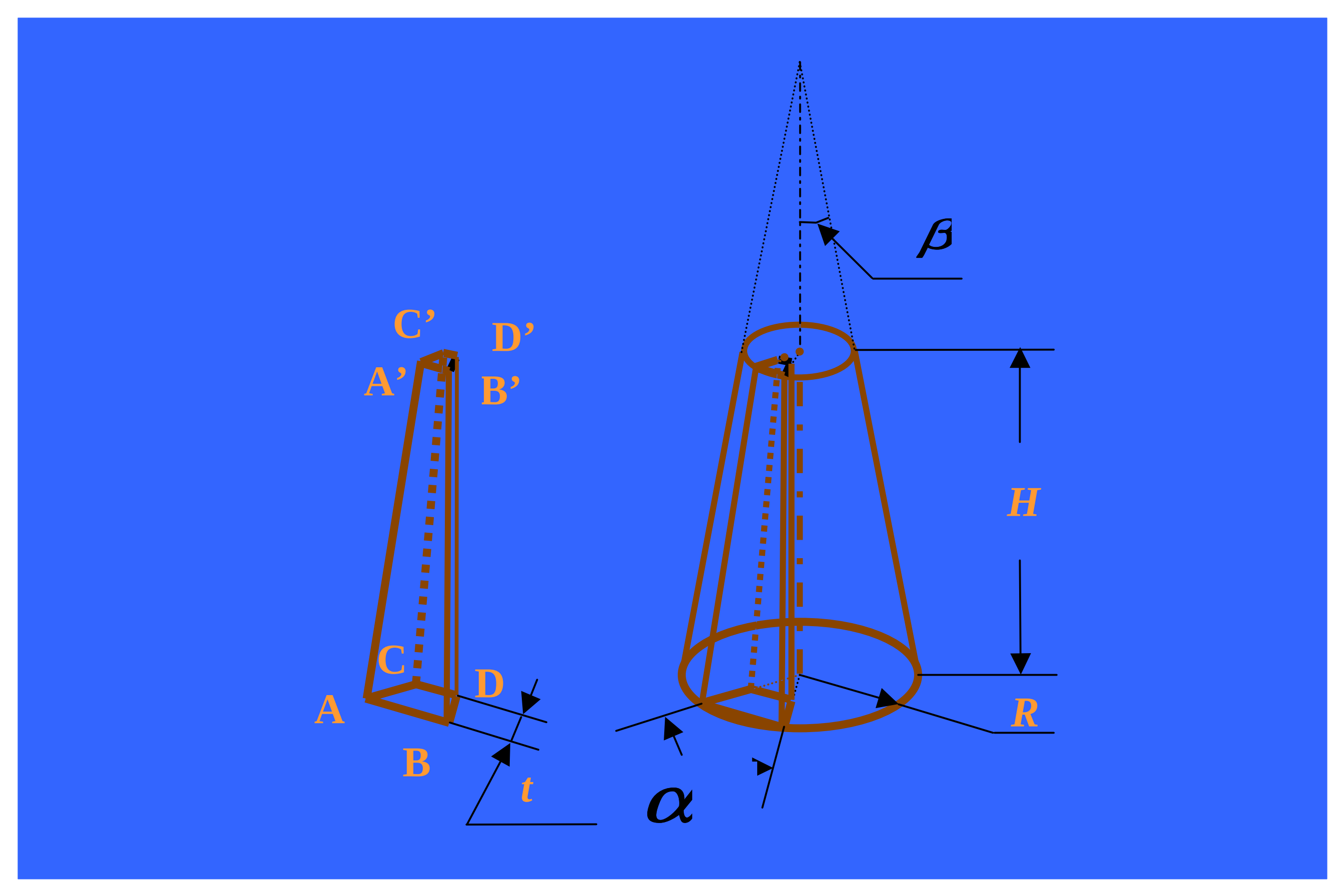

Materials

- Southern Yellow Pine
- Resorcinol-Phenol-Formaldehyde (RPF) Resin

Experimental Design

- Reduced-size Composite Poles
  - Diameter: 3 in.
  - Length: 48 in.
  - Strip Number: 6   9   12
  - Strip Thickness: 0.4   0.6   0.8   1.0 in.

Experimental Design (Cont.)

- Full-Size Composite Poles
  - Diameter: 4 in.
  - Length: 20 ft.
  - Strip Number: 9   12
  - Strip Thickness: 0.75   1.125   1.5 in.

Methods

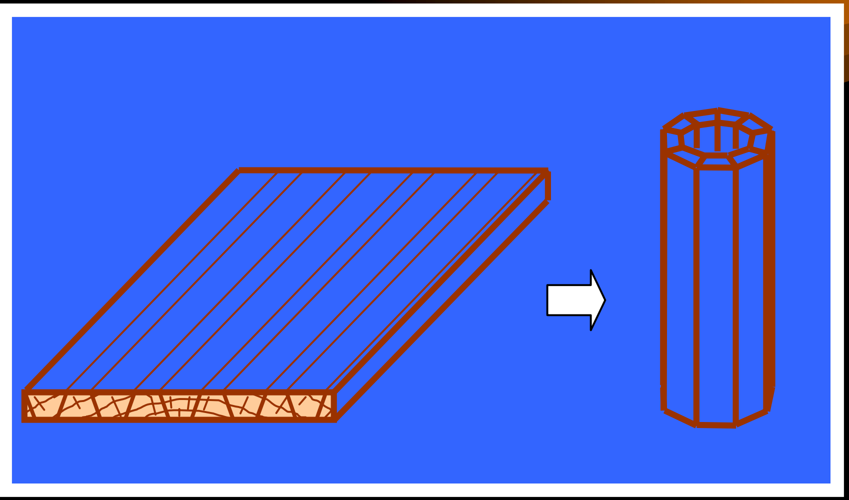

Processing of Full-Size Poles

Testing of Reduced-Size Poles

Testing of Full-Size Poles

Testing of Shear Strength

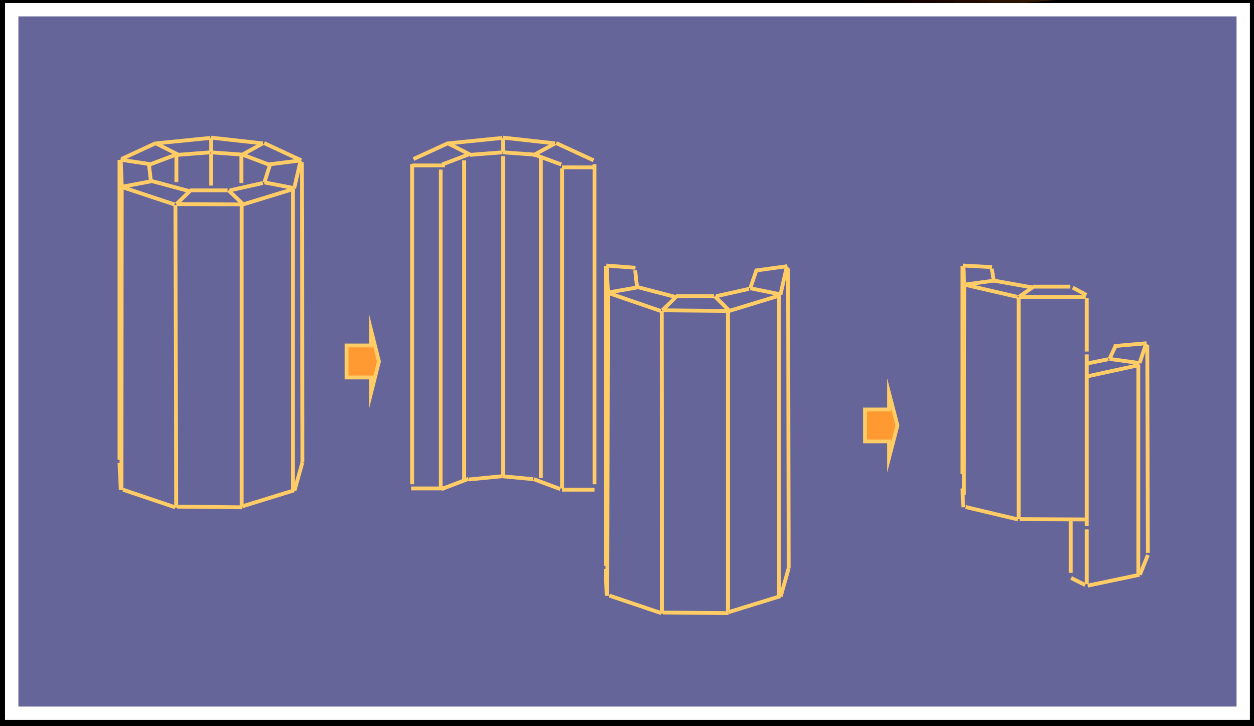

MOR of Composite Poles

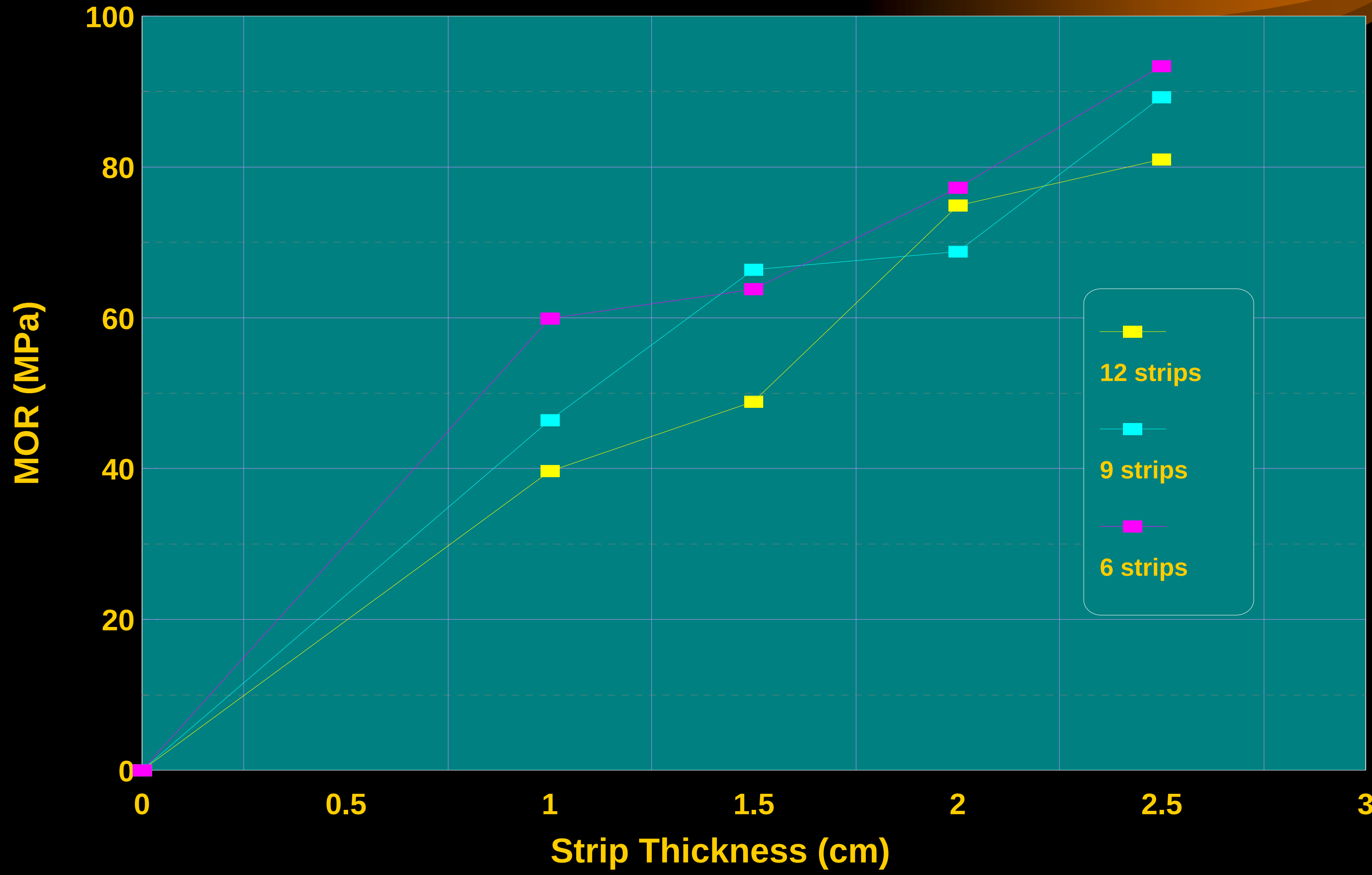

MOE of Composite Poles

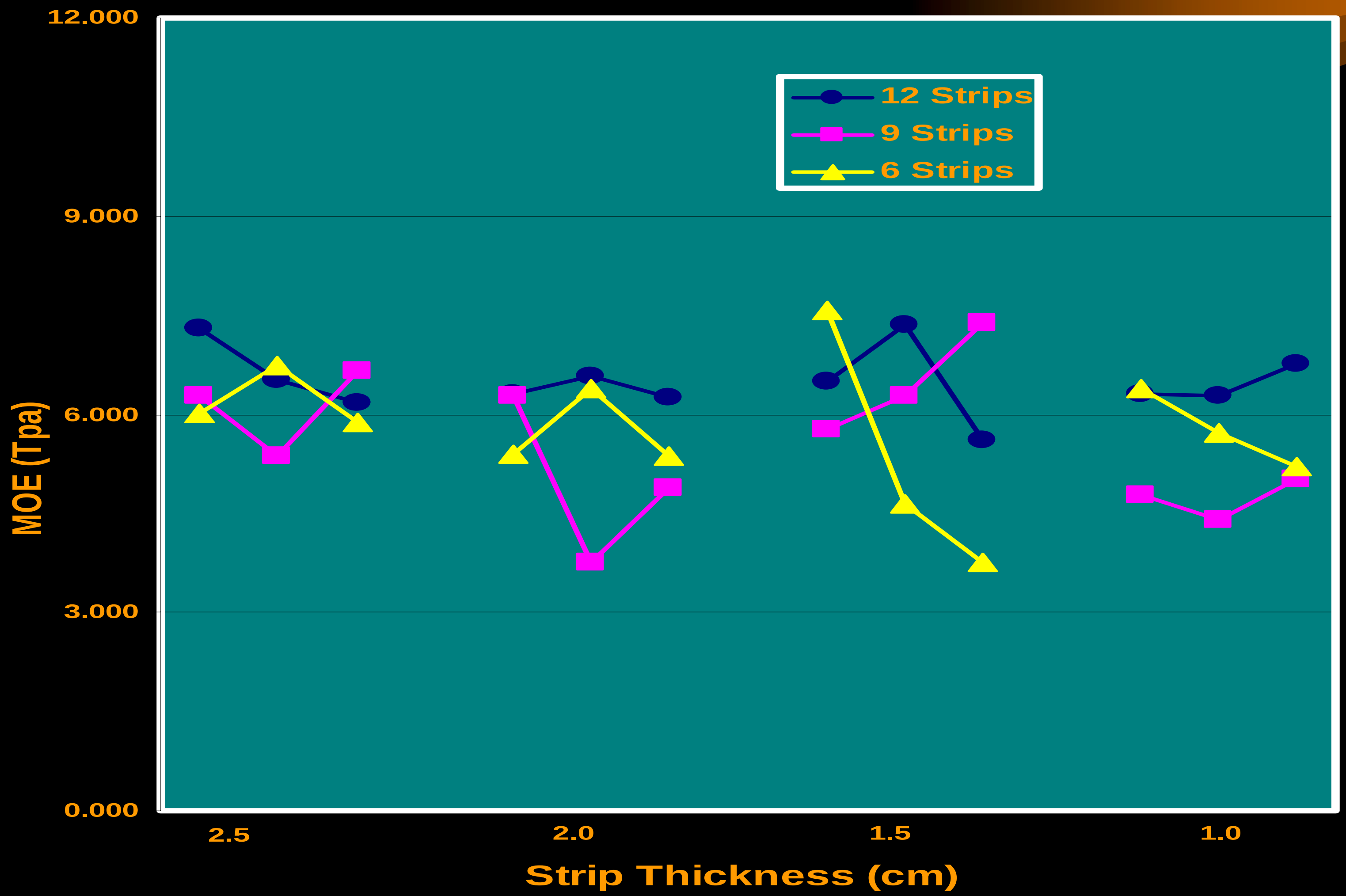

Glue-Line Shear in the Dry Condition

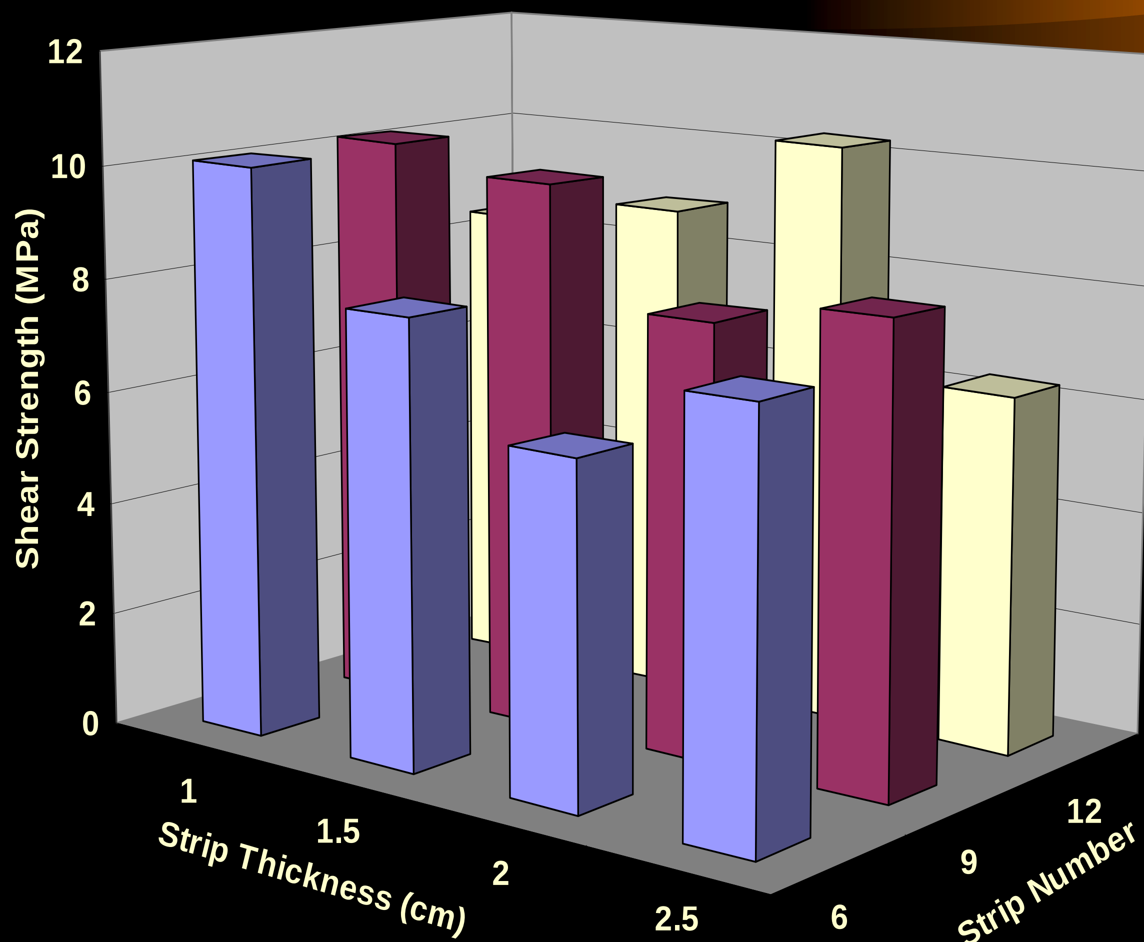

Glue-Line Shear in the Wet Condition

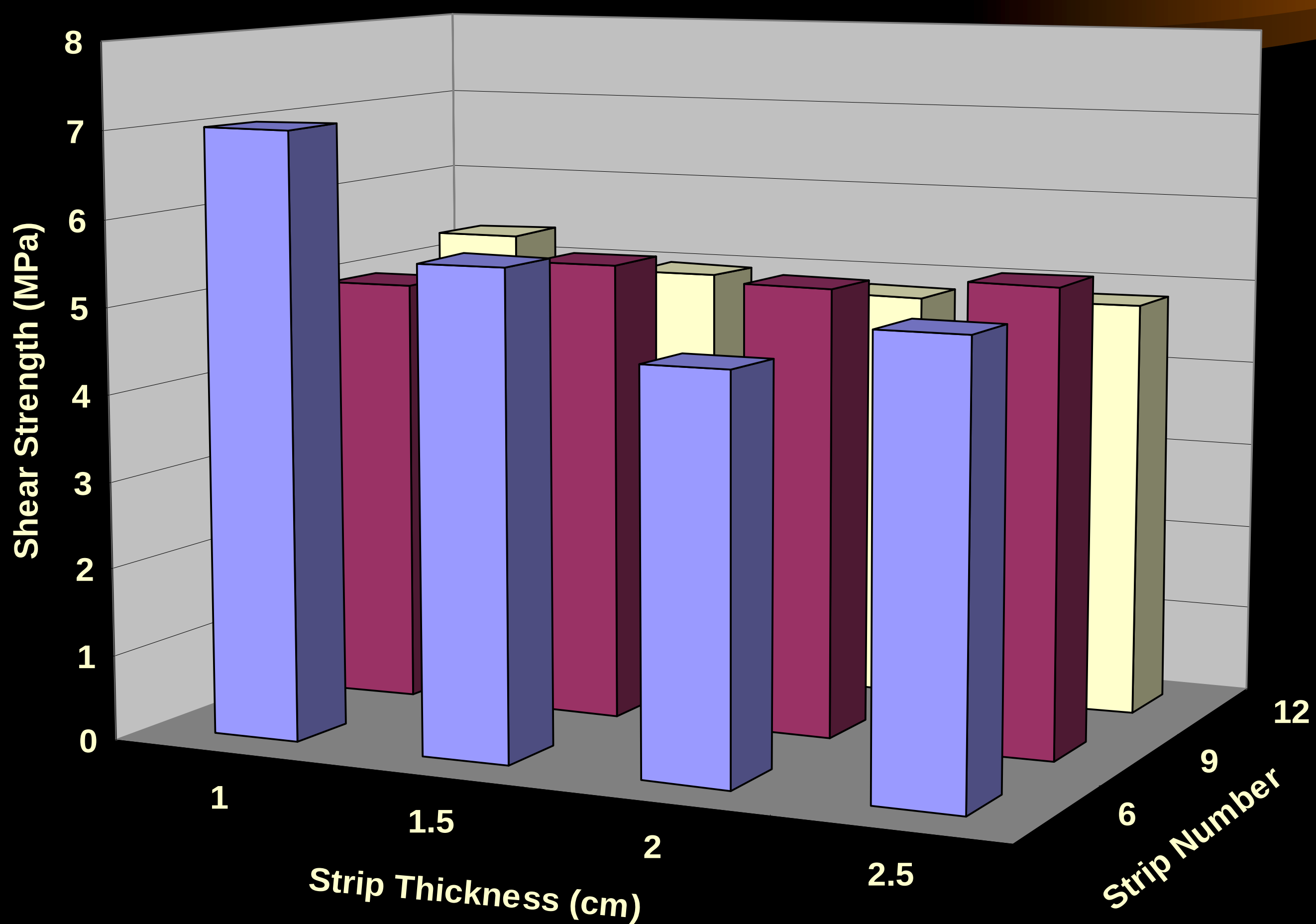

Wood Breakage in the Dry Condition

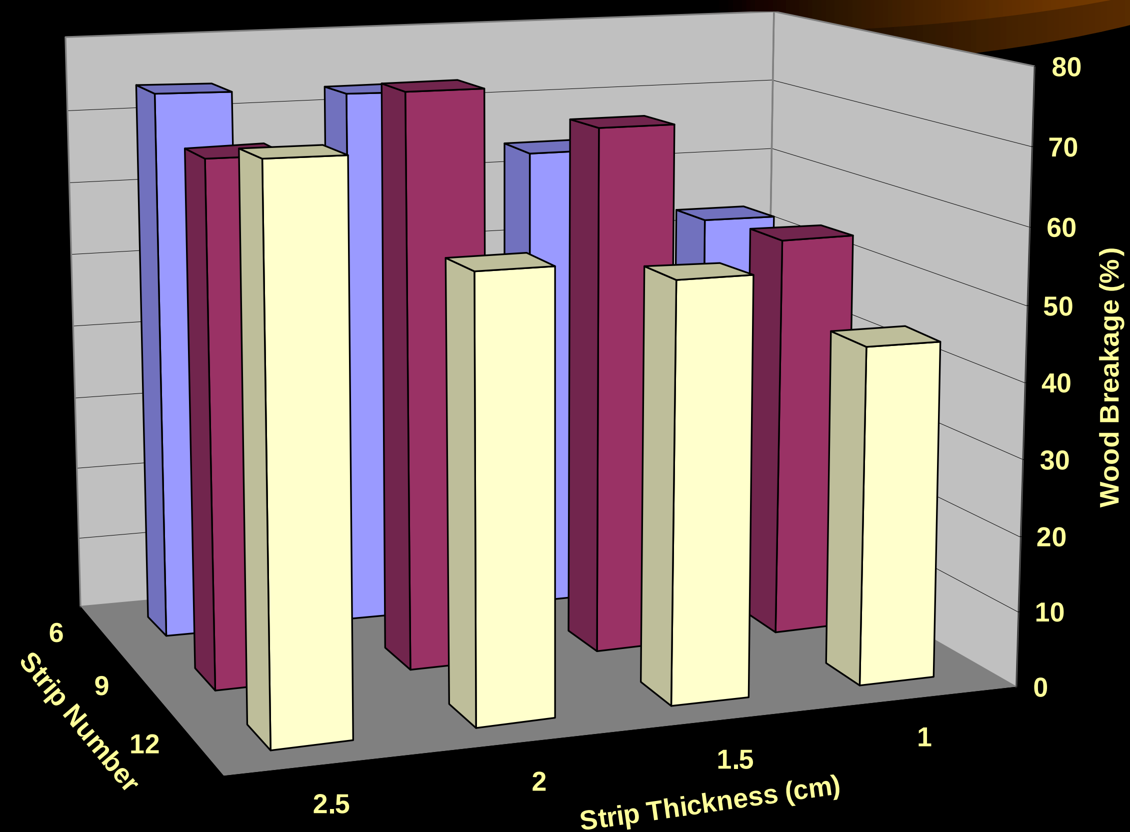

Wood Breakage in the Wet Condition

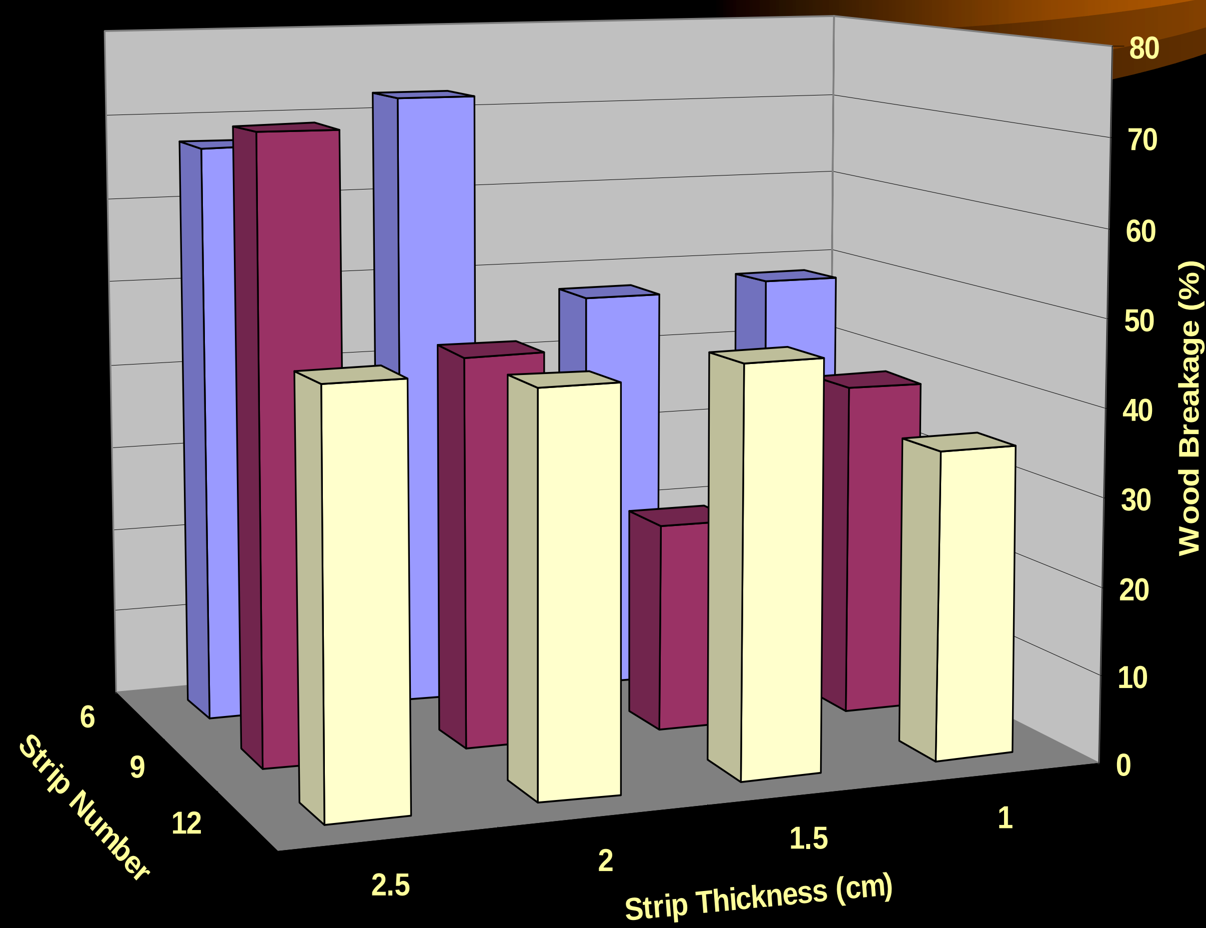

Conclusions

- Strip thickness positively affects maximum stress and negatively affects glue-line shear strength. Strip thickness was not correlated with the Young's modulus.

Conclusions (cont.)

- Maximum stress decreased, and Young's modulus increased with strip number. Strip number had no effects on glue-line shear strength.

Conclusions (cont.)

- The boiling treatment resulted in reduction in shear strength and increased wood failure. Thinner strips lose more shear strength after the treatment.

Conclusions (cont.)

- Young’s modulus of reduced-size composite poles was inferior to that of solid poles, whereas Young’s modulus of full-size poles was superior to solid poles.

Theoretical Analysis

Loading system and shear and moment distributions

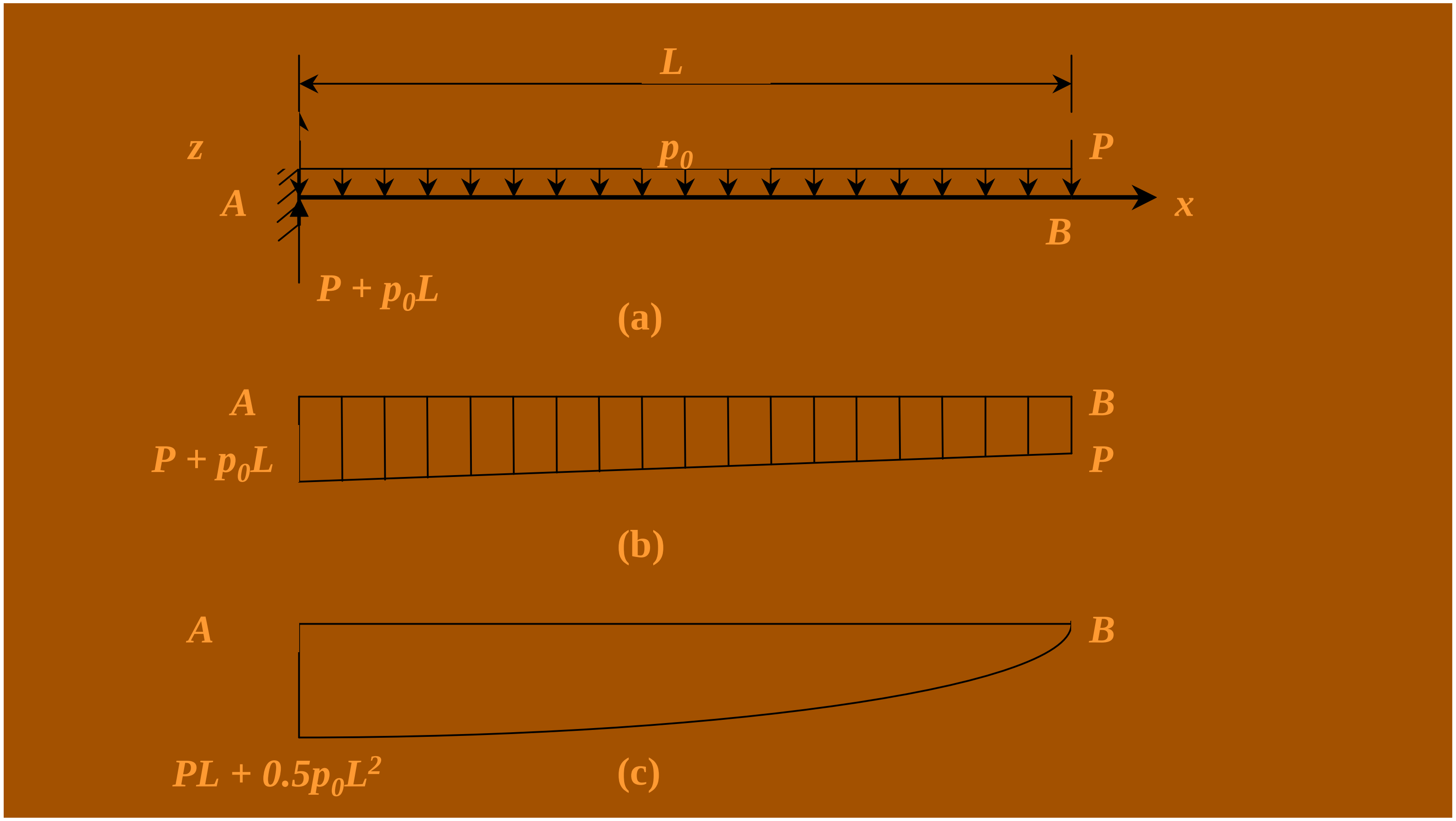

Normal and Shear Stresses

$$\sigma_x = \frac{Mz}{I}$$

$$\tau_{xy} = \frac{dM}{dx}\frac{1}{bI}\int_z^R z\,dA = \frac{VQ}{Ib}$$

Normal and Shear Strains

$$\varepsilon_x = \frac{du_x}{dx} = -z\frac{d^2w}{dx^2}$$

$$\gamma_{xy} = \frac{\tau_{xy}}{G}$$

Strain Energy Functions

$$W_\sigma = \frac{1}{2}\sigma_x \varepsilon_x = \frac{1}{2}E\varepsilon_x^2 = \frac{1}{2}E(\frac{d^2w}{dx^2})^2 z^2$$

$$W_\tau = \frac{1}{2}\frac{V^2Q^2}{GI^2b^2} = \frac{1}{2}\frac{E^2Q^2}{Gb^2}(\frac{d^3w}{dx^3})^2$$

Normal and Shear Strain Energies

$$U_\sigma = \frac{EI}{2}\int_0^L \left(\frac{d^2w}{dx^2}\right)^2 dx$$

$$U_\tau = \frac{E^2}{2G}\int_0^L \left(\frac{d^3w}{dx^3}\right)^2 dx \int_A \frac{Q^2}{b^2} dydz = \frac{k_1 E^2}{2G}\int_0^L \left(\frac{d^3w}{dx^3}\right)^2 dx$$

Glue-Line Effects

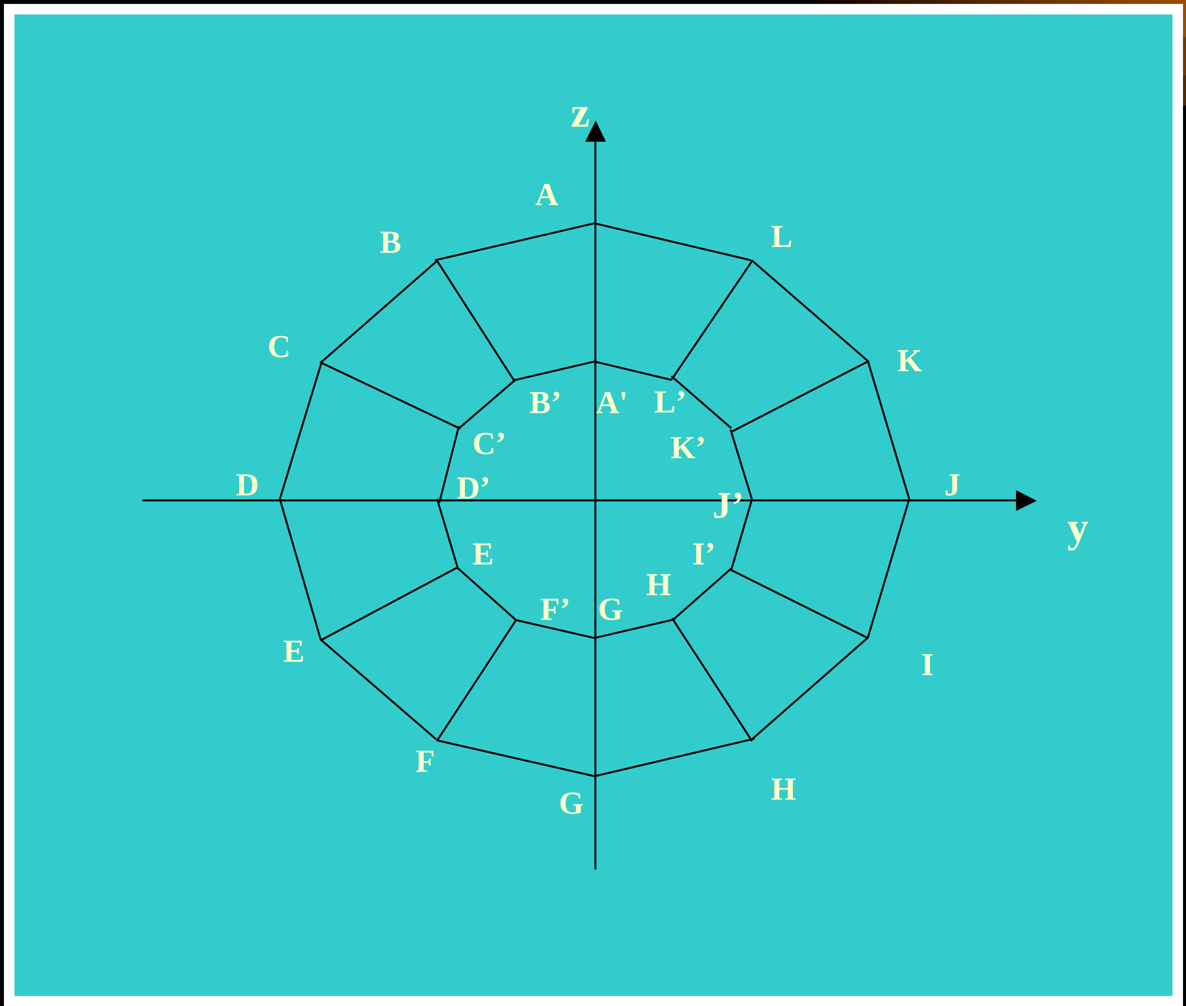

Glue-Line Energy

$$U_g = 2U_{AA'} + 4U_{BB'} + 4U_{CC'} + 2U_{DD'}$$

$$= k_6 \int_0^L \left(\frac{d^2w}{dx^2}\right)^2 dx + k_7 \int_0^L \left(\frac{d^3w}{dx^3}\right)^2 dx$$

$$k_6 = E_g(I_{g1} + 2I_{g2} + 2I_{g3})$$

$$k_7 = k_5(k_1 + k_2 + k_3 + k_4)$$

$$k_5 = \frac{E_g^2}{2G_g}$$

$$k_4 = 2\iint_A \frac{Q_{g1}^2}{t^2 I_{g1}} dA$$

$$k_3 = 4\iint_A \frac{Q_{g2}^2}{t^2 I_{g2}} dA$$

$$k_2 = 4\iint_A \frac{Q_{g3}^2}{t^2 I_{g3}} dA$$

$$k_1 = 2\iint_A \frac{Q_{g4}^2}{t^2 I_{g4}} dA$$

External Energy

$$H = -\int_0^L p_0 w dx - Pw(L)$$

Total Potential Energy

$$\pi = U_\sigma + U_\tau + U_g + H$$

$$= k_8 \int_0^L \left(\frac{d^2 w}{dx^2}\right)^2 dx + k_9 \int_0^L \left(\frac{d^3 w}{dx^3}\right)^2 dx - \int_0^L p_0 w dx - Pw(L)$$

$$k_8 = \frac{1}{2} EI + k_6$$

$$k_9 = \frac{k_1 E^2}{2G} + k_7$$

Application of Minimum Potential Energy Theorem

$$\delta\pi = \frac{\partial \pi}{\partial x} dx = 0$$

$$k_8 \int_0^L 2\frac{d^2 w}{dx^2}\delta\left(\frac{d^2 w}{dx^2}\right)dx + k_9 \int_0^L 2\frac{d^3 w}{dx^3}\delta\left(\frac{d^3 w}{dx^3}\right)dx - \int_0^L p_0 \delta w dx - P\delta w(L) = 0$$

The Governing Differential Equation

$$\boxed{k_9 \frac{d^6 w}{dx^6} + k_8 \frac{d^4 w}{dx^4} - \frac{p_0}{2} = 0}$$

Boundary Conditions

$$[k_9 \frac{d^5 w}{dx^5} - k_8 \frac{d^3 w}{dx^3})]|_{x=L} = \frac{P}{2}$$

$$w|_{x=0} = 0$$

$$(k_8 \frac{d^2 w}{dx^2} - k_9 \frac{d^4 w}{dx^4})|_{x=L} = 0$$

$$w'|_{x=0} = 0$$

$$k_8 \frac{d^3 w}{dx^3}|_{x=0} = 0$$

$$k_8 \frac{d^2 w}{dx^2}|_{x=L} = 0$$

Solution

$$w = c_1 + c_2 x + c_3 x^2 + c_4 x^3 + \frac{1}{48k_8} p_0 x^4 + c_5 e^{k_{10} x} + c_6 e^{-k_{10} x}$$

$$k_{10} = \sqrt{\frac{k_8}{k_9}}$$

High-order differential equation: deflection of reduced-size poles

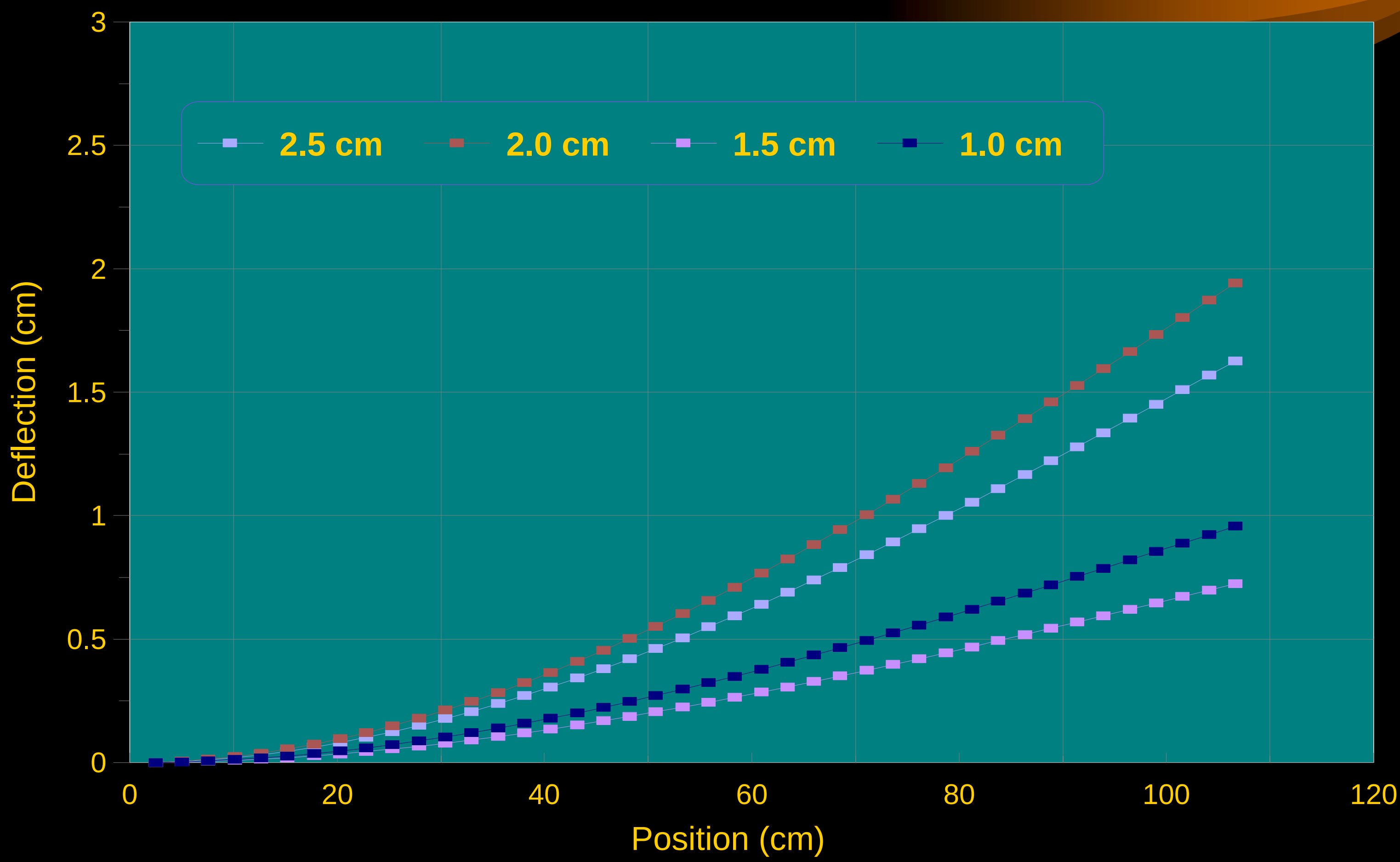

High-order differential equation: Deflection of full-size poles

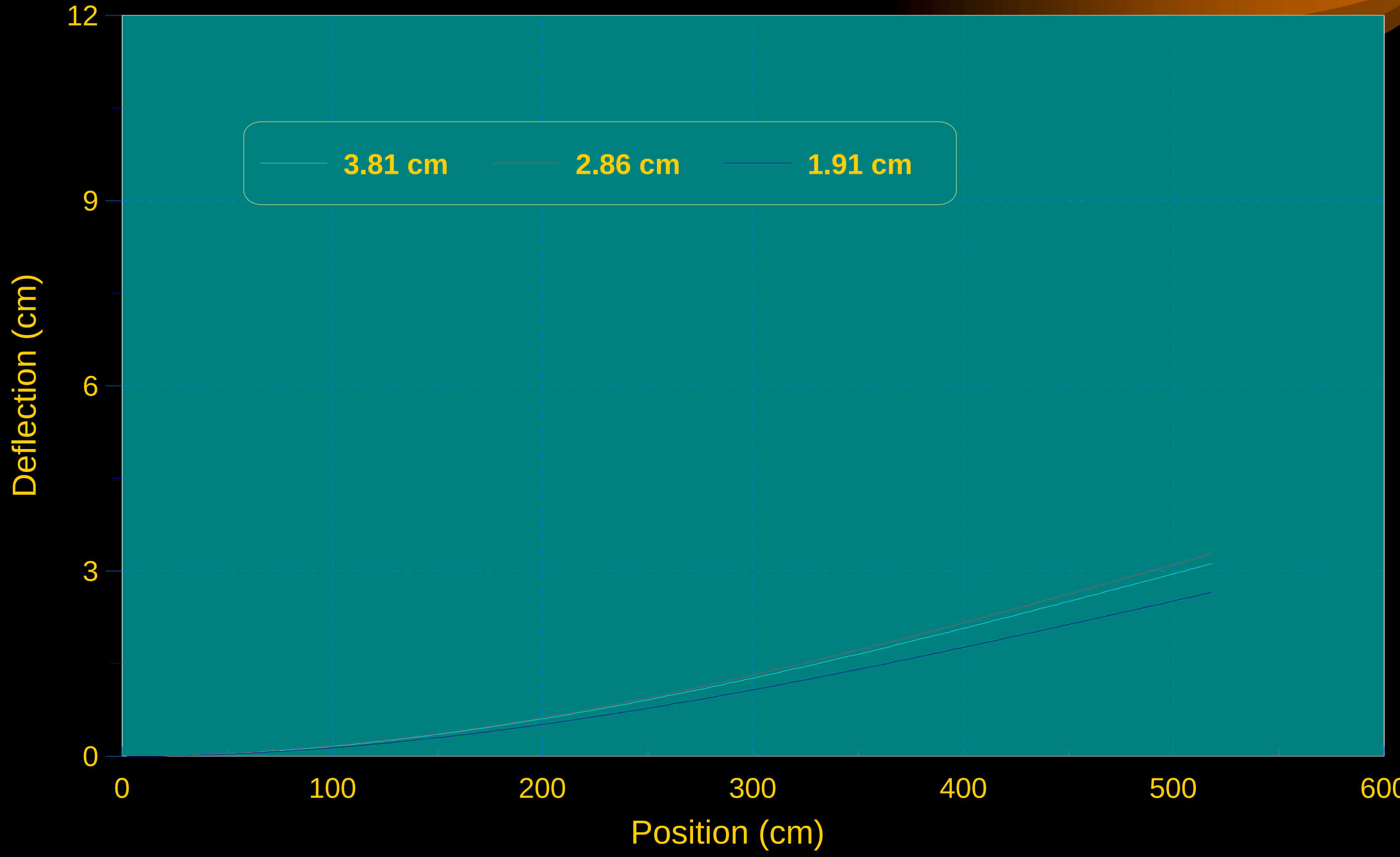

Comparison between high-order differential equation and Timoshenko methods: reduced-size poles

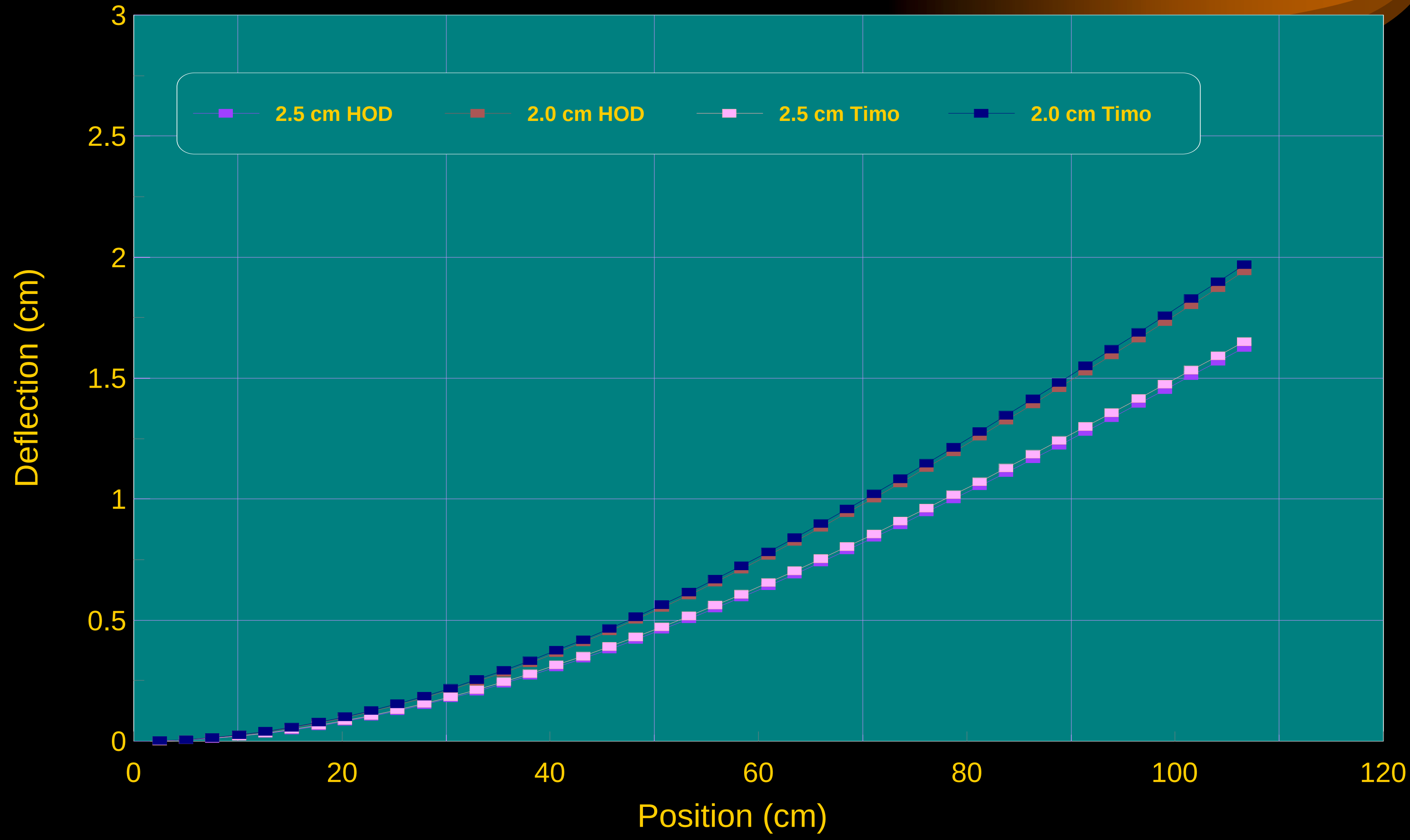

Comparison between high-order differential equation and Timoshenko methods: full-size poles

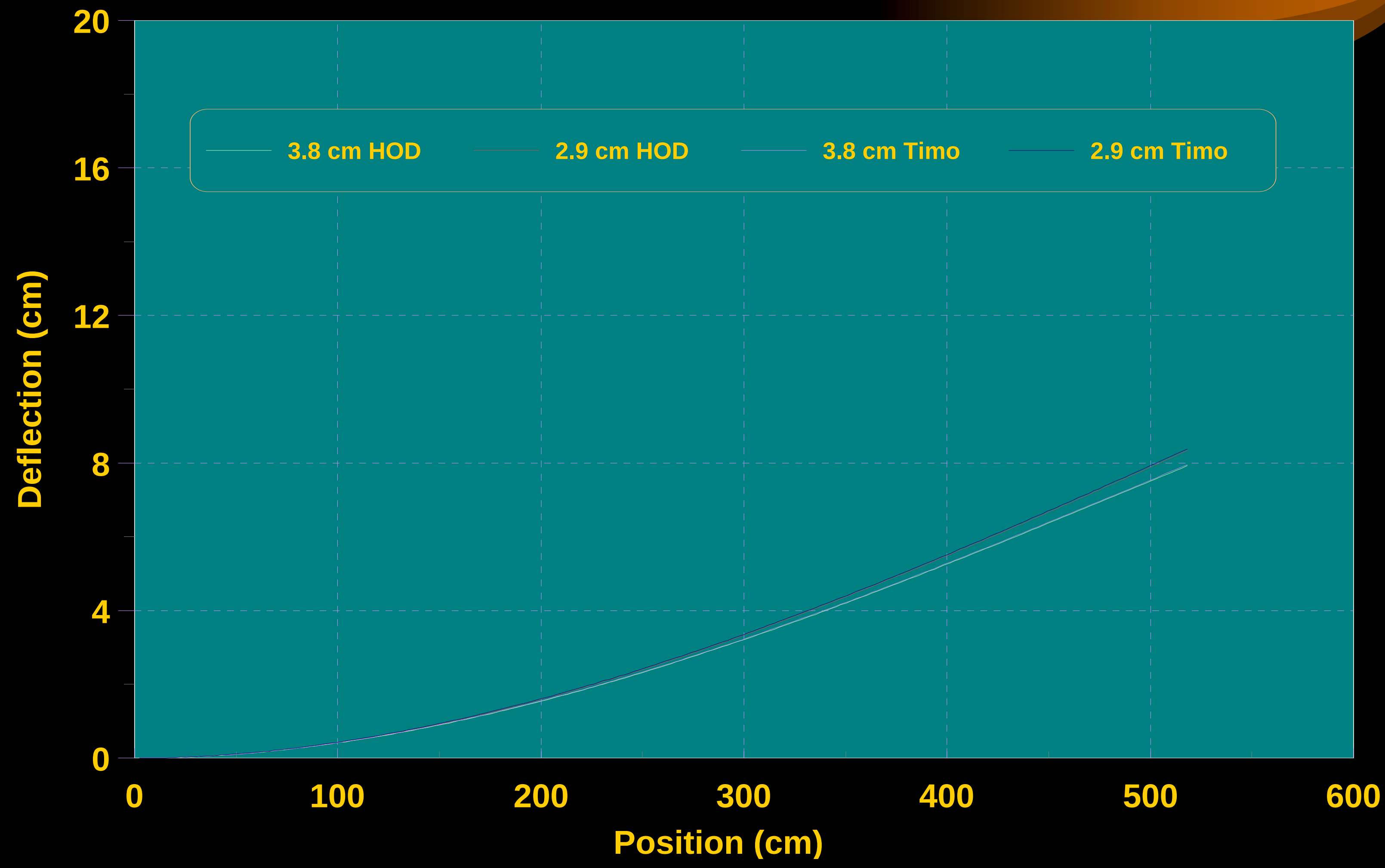

Shear Effects on Deflection

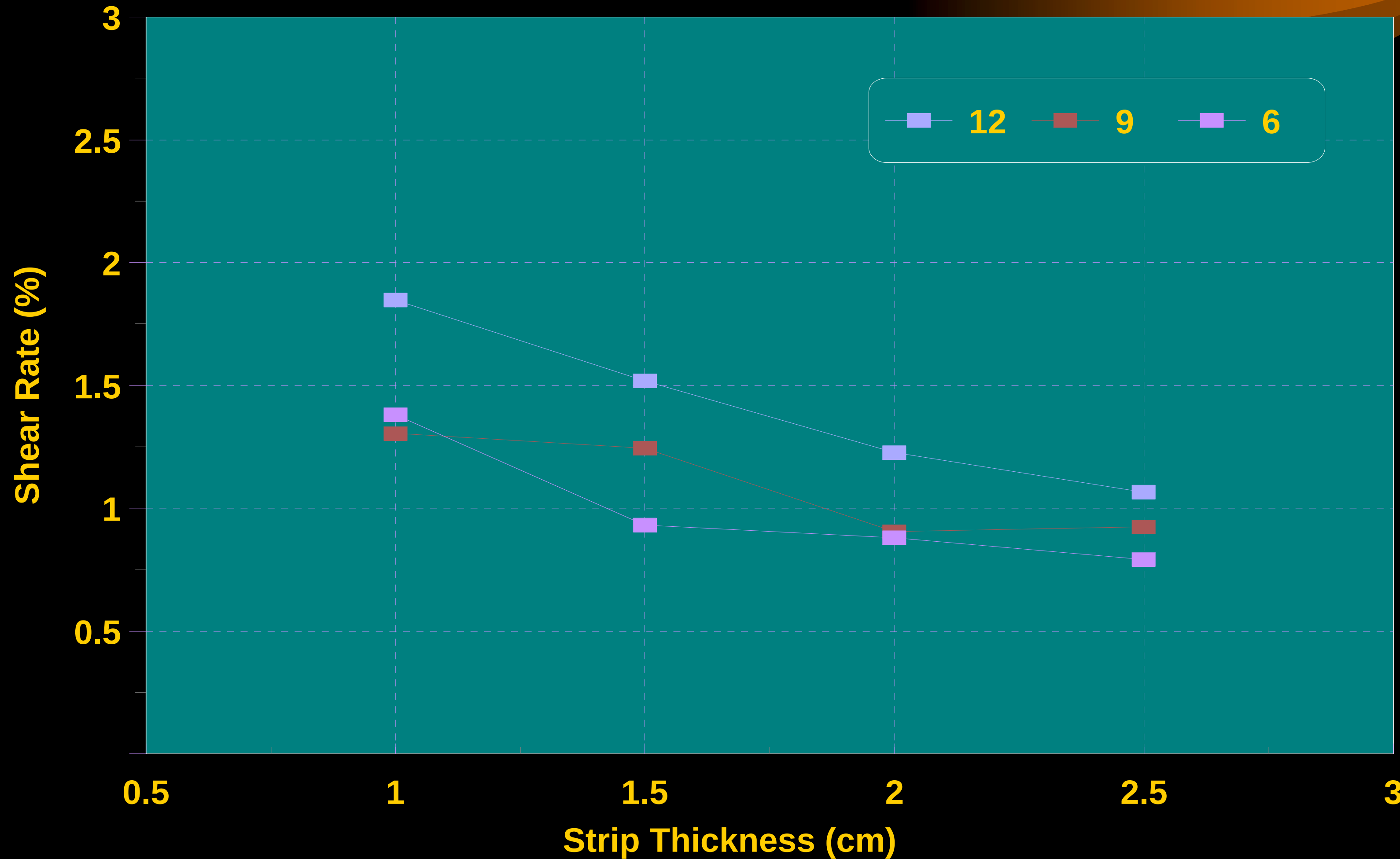

Deflection Comparison between Experiment Results and Theoretical Models

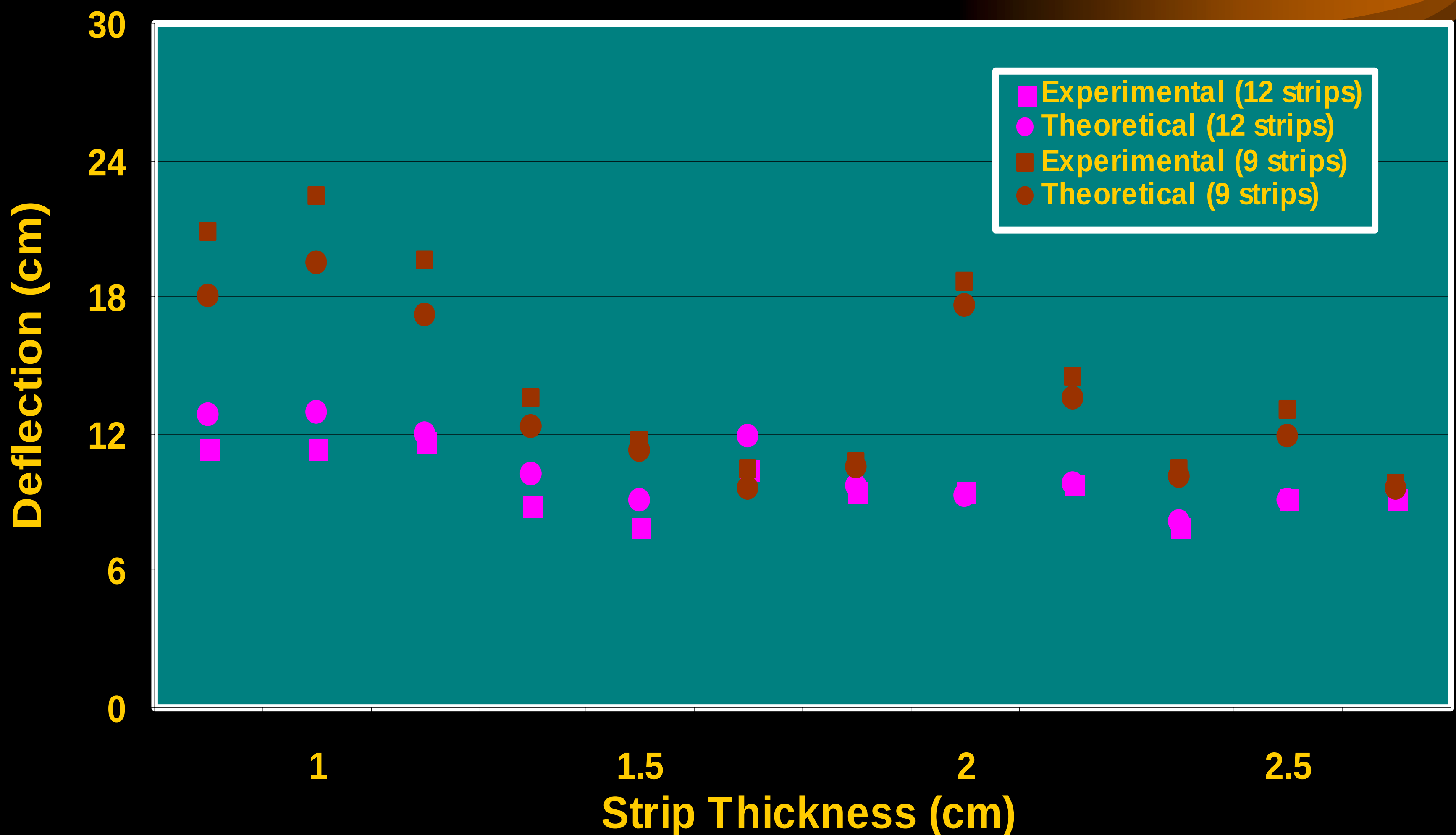

Stress Distribution

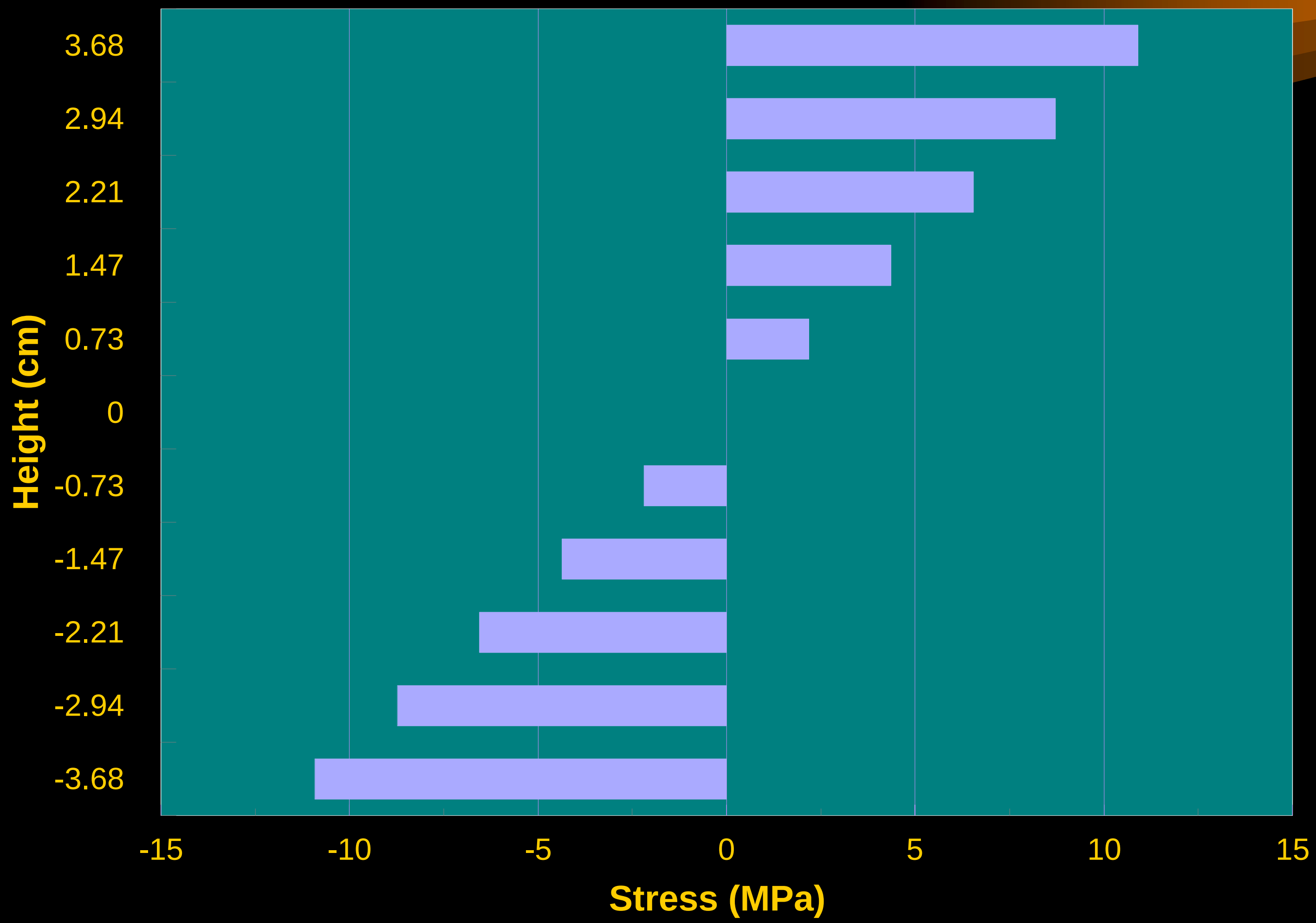

Conclusions of Theoretical Analysis

- A theoretical model was developed
- The high-order differential model was more accurate than the Timoshenko model in the prediction of full-size poles

Conclusions of Theoretical Analysis (cont.)

- Shear deflection account for 1 to 2% of the total deflection for reduced-size composite poles, and 0.1 to 1% for full-size composite poles

- Glue-line deflection accounted for 4% of the total deflection for reduced-size poles, and 5% for full-size composite poles

Finite Element Analysis

Discretization of Domain: Reduced-Size Poles

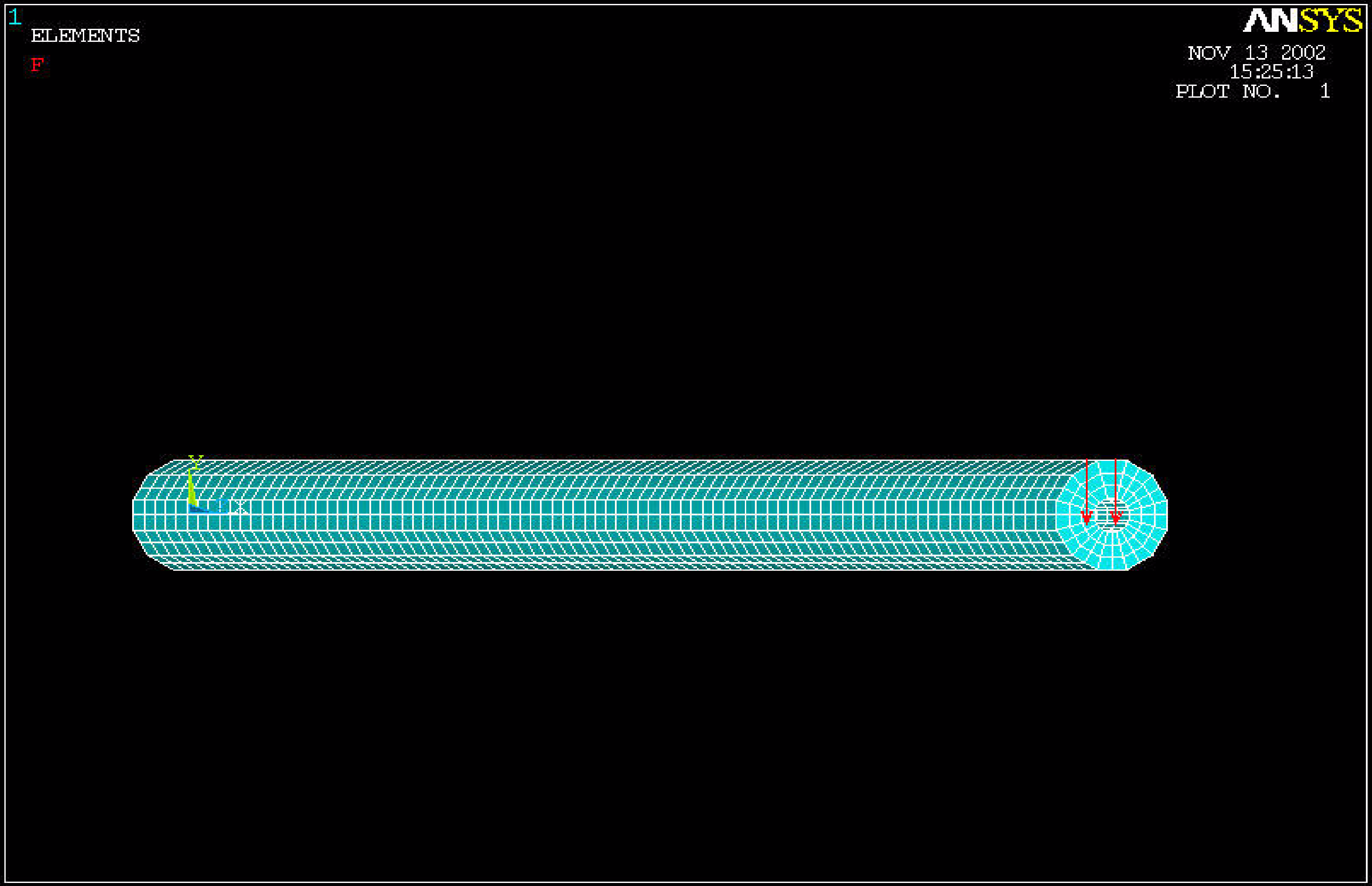

Discretization of Domain: Full-Size Poles

Element Numbering for A 12-Side Pole

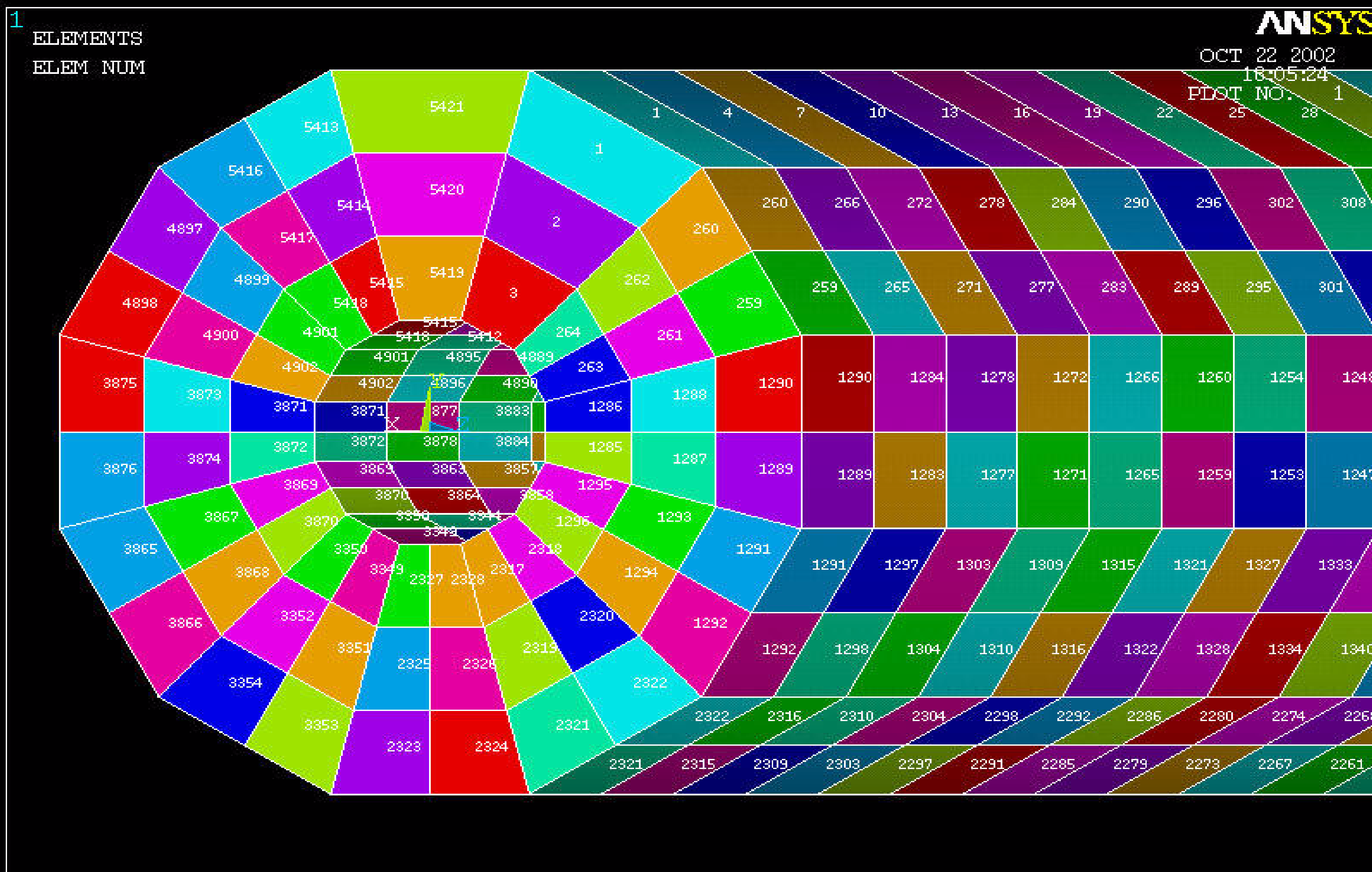

Node Numbering for A 12-Side Pole

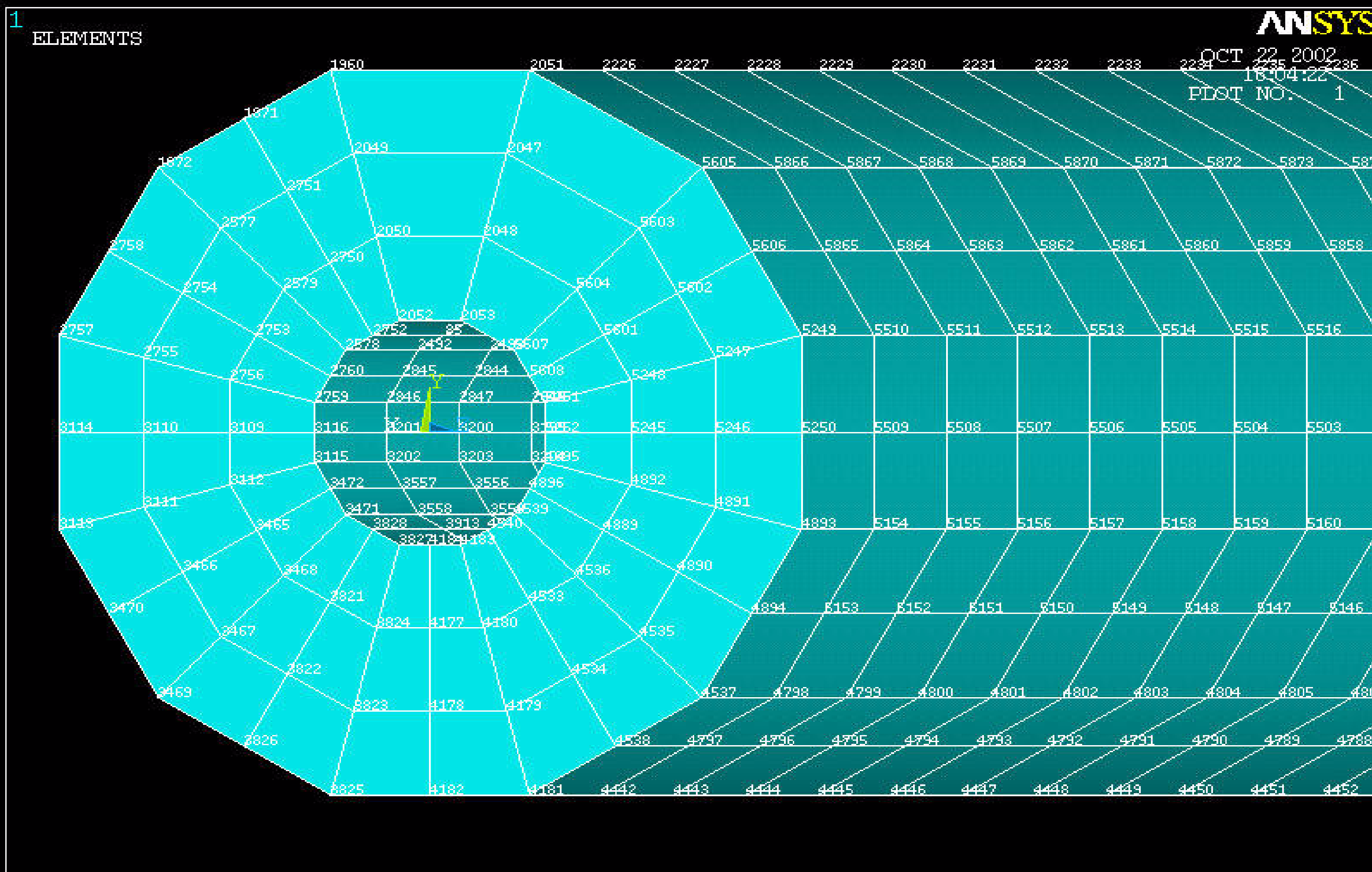

Element Numbering for 6-Side Pole

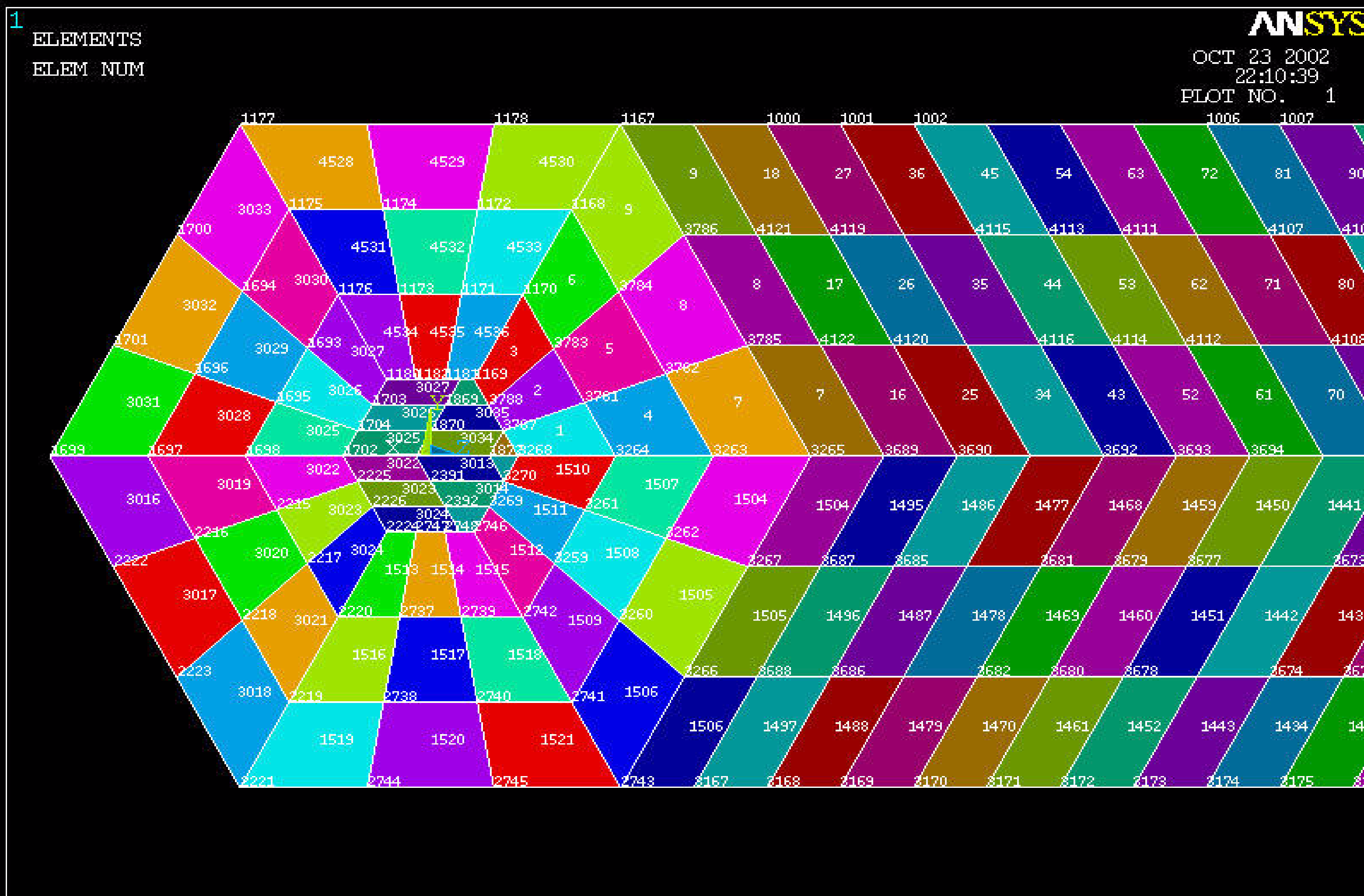

Deformation of A 12-Side Small Pole

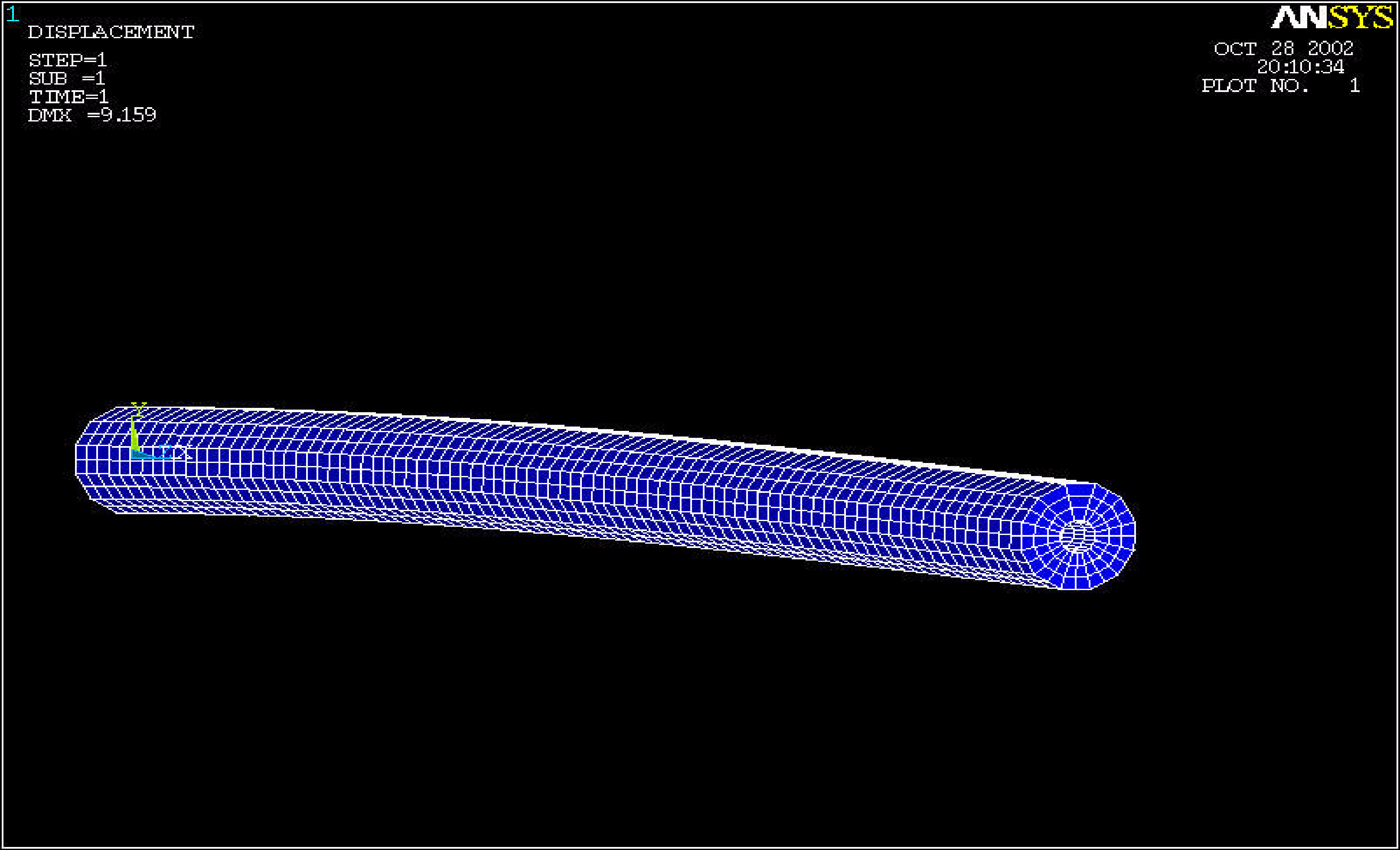

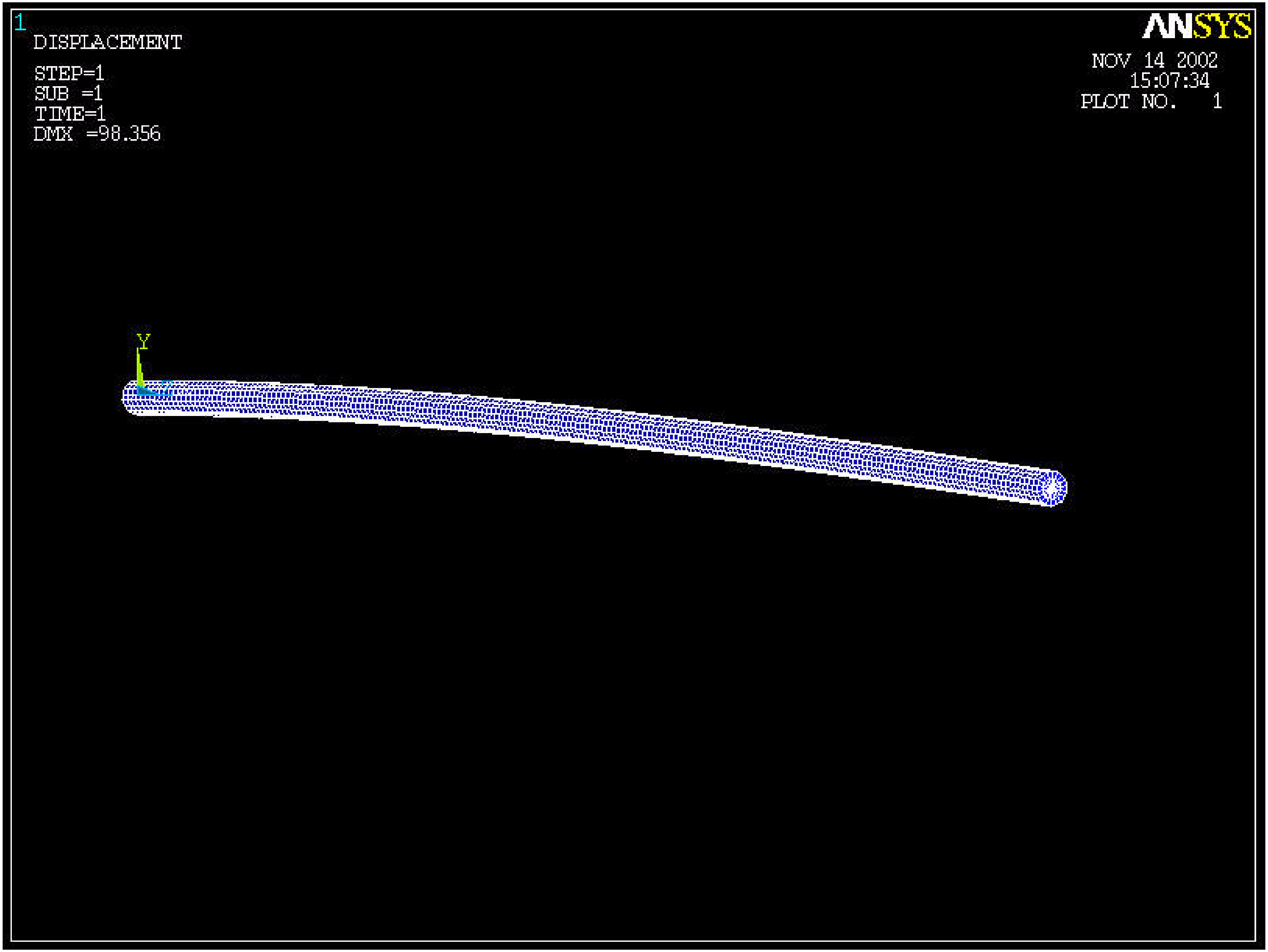
1
DISPLACEMENT
STEP=1
SUB =1
TIME=1
DMX =98.356
ANSYS
NOV 14 2002
15:07:34
PLOT NO. 1
Y

Stress Distribution of A 12-Side Pole

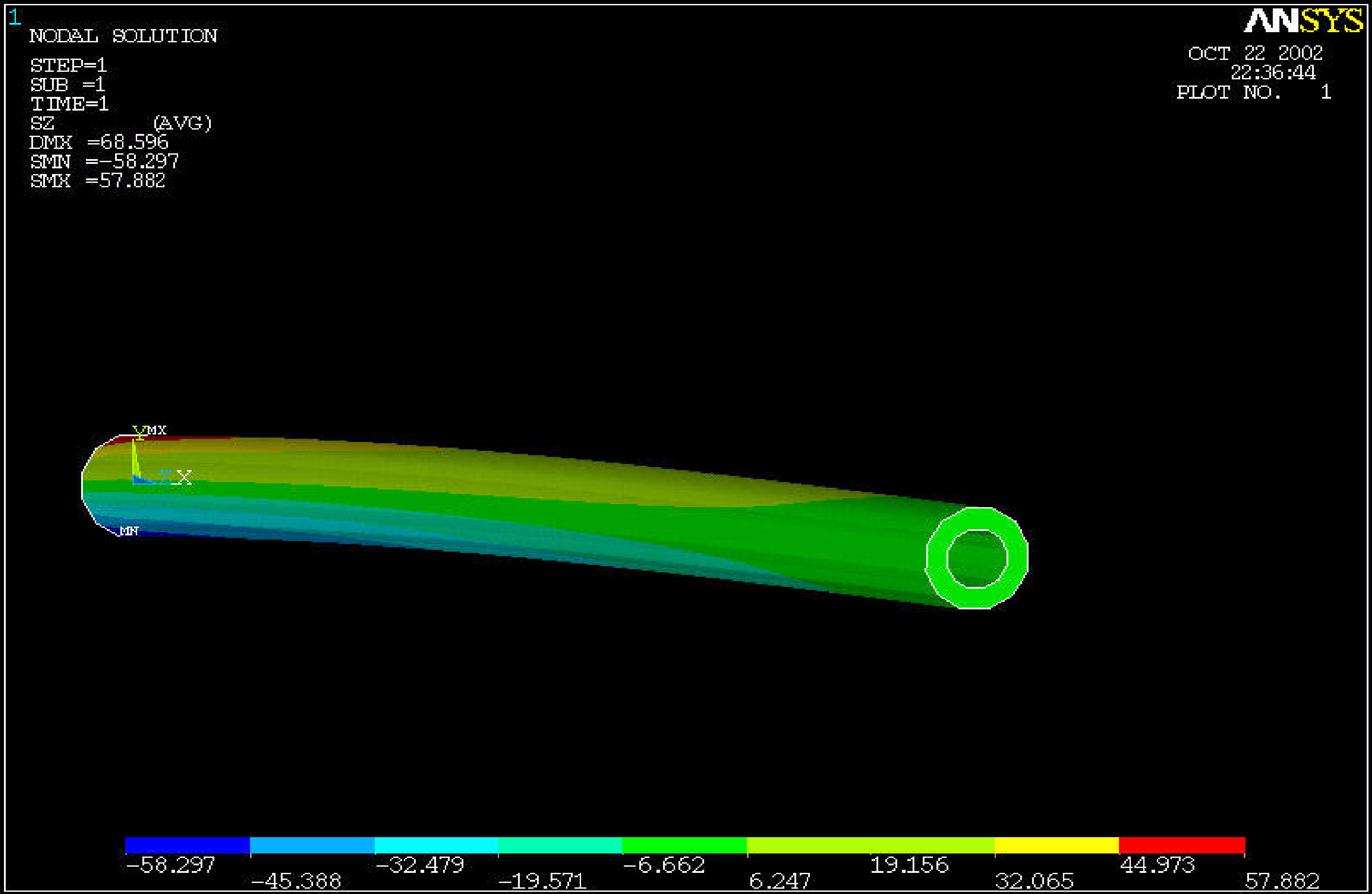

Stress Distribution of A 12-Side Full-Size Pole

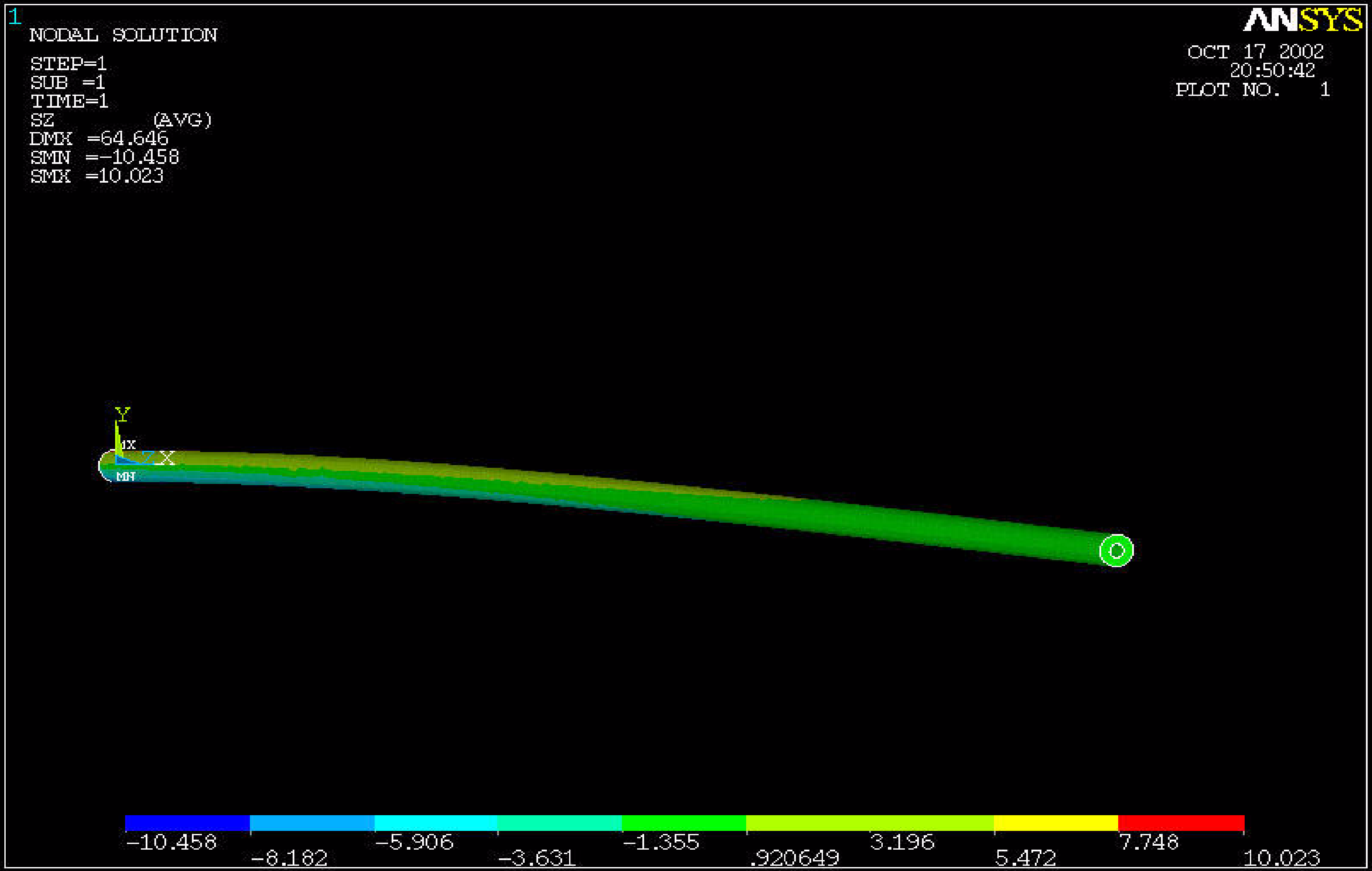

Strain Distribution of A 12-Side Full-Size Pole

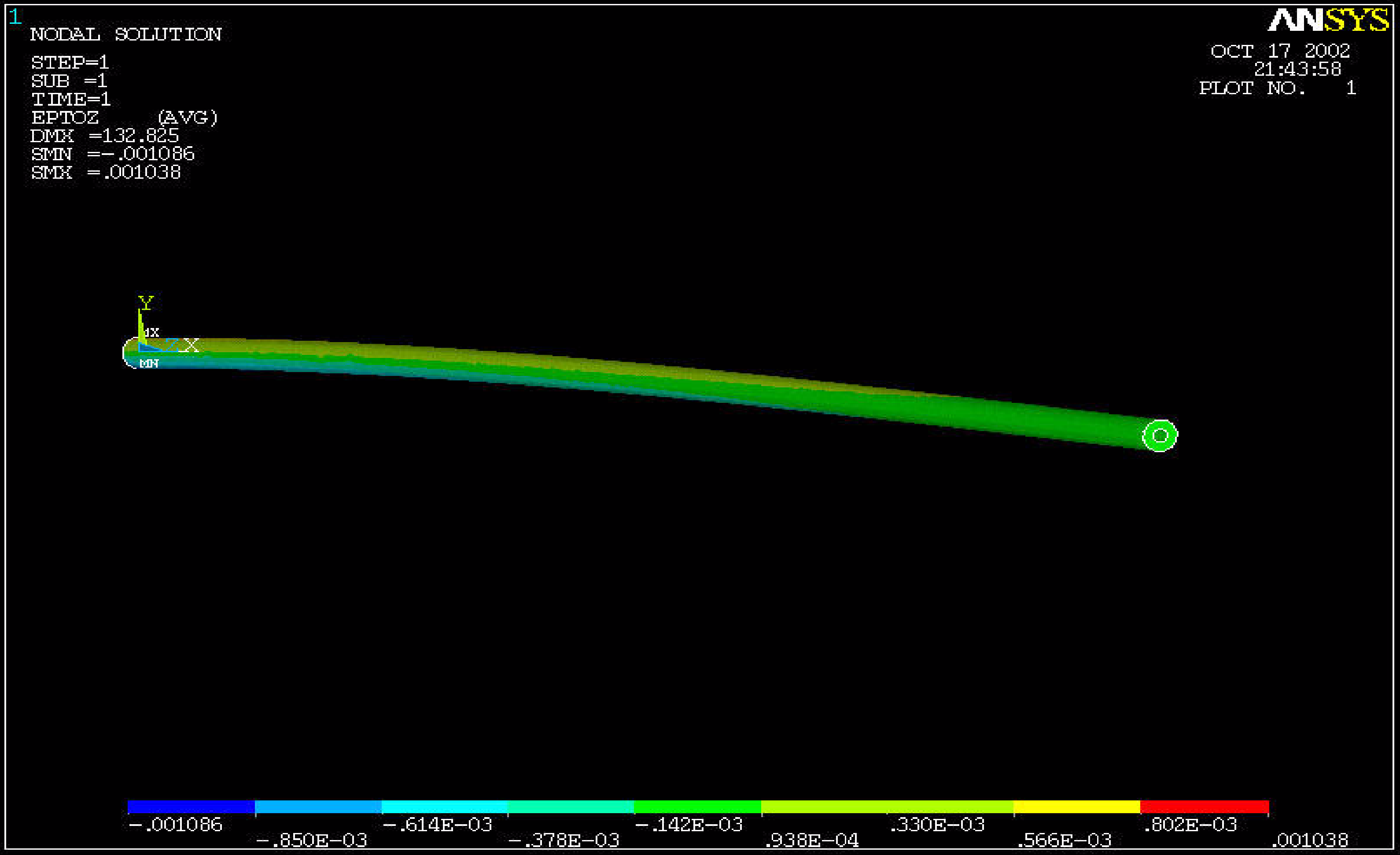

FEM-Predicted Deflection of 12-Side Reduced-Size Composite Poles

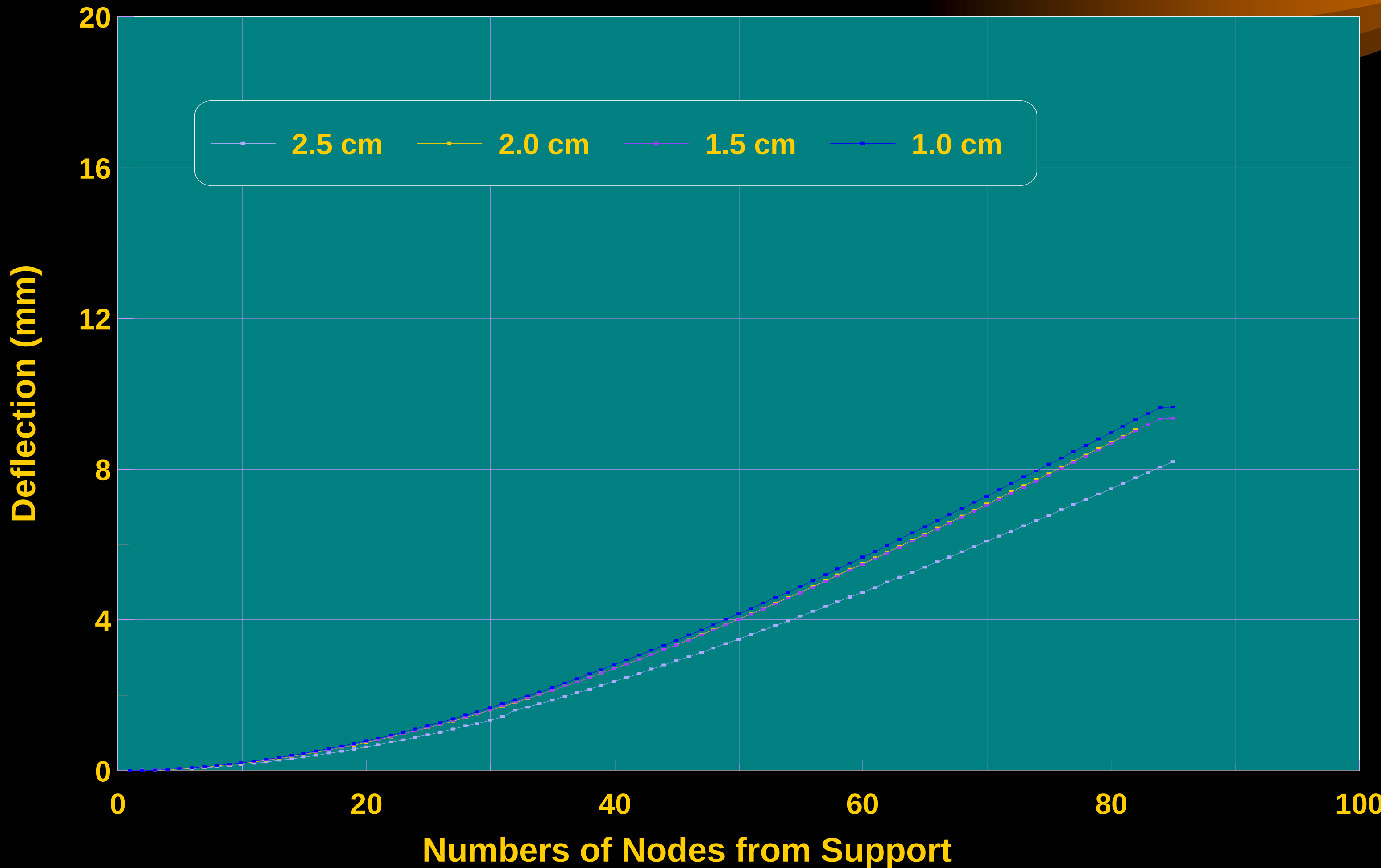

FEM-Predicated Deflection of 12-Strip Full-Size Composite Poles

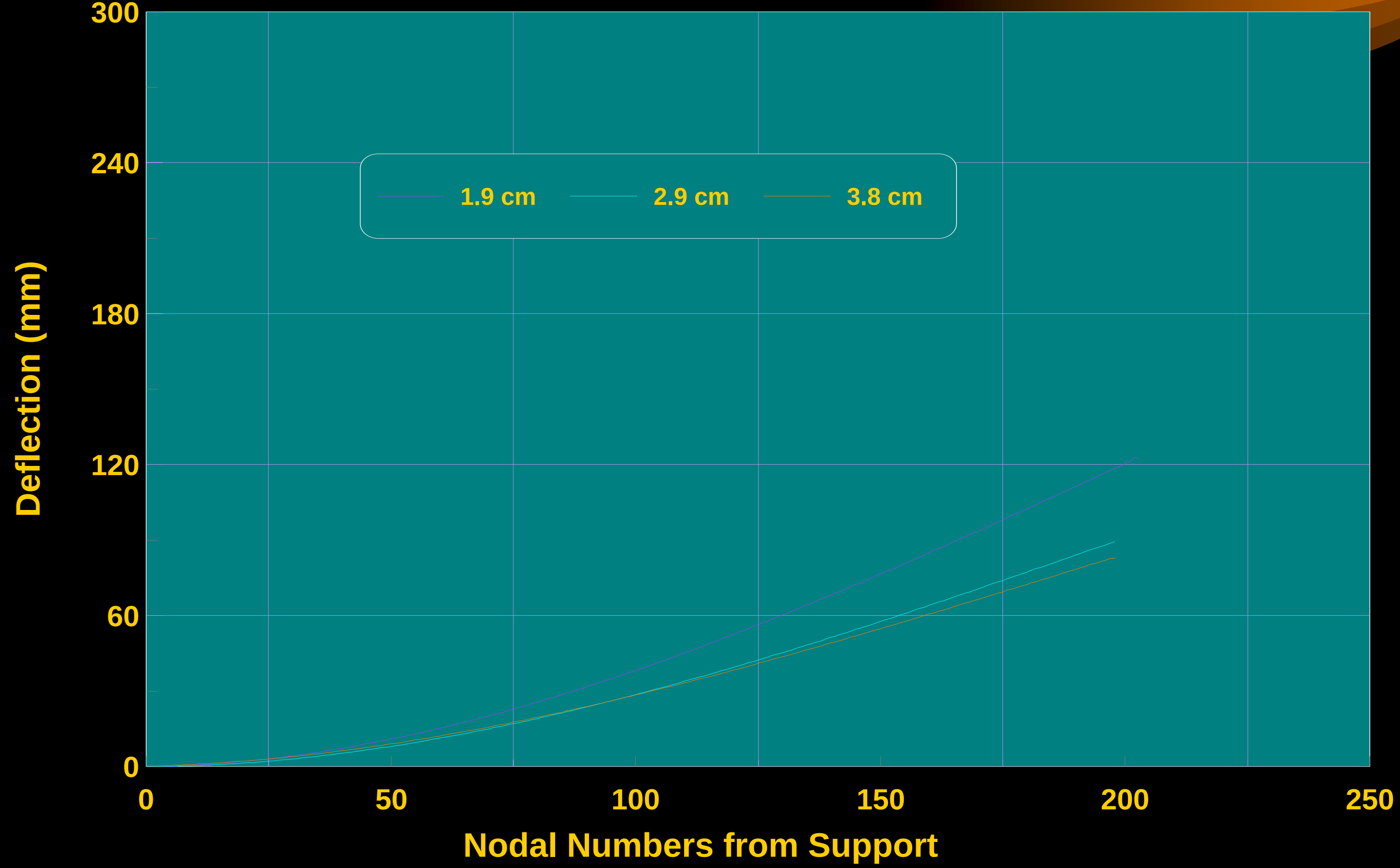

FEM-Predicted Maximum Stress of 12-Side Reduced-Size Composite Poles

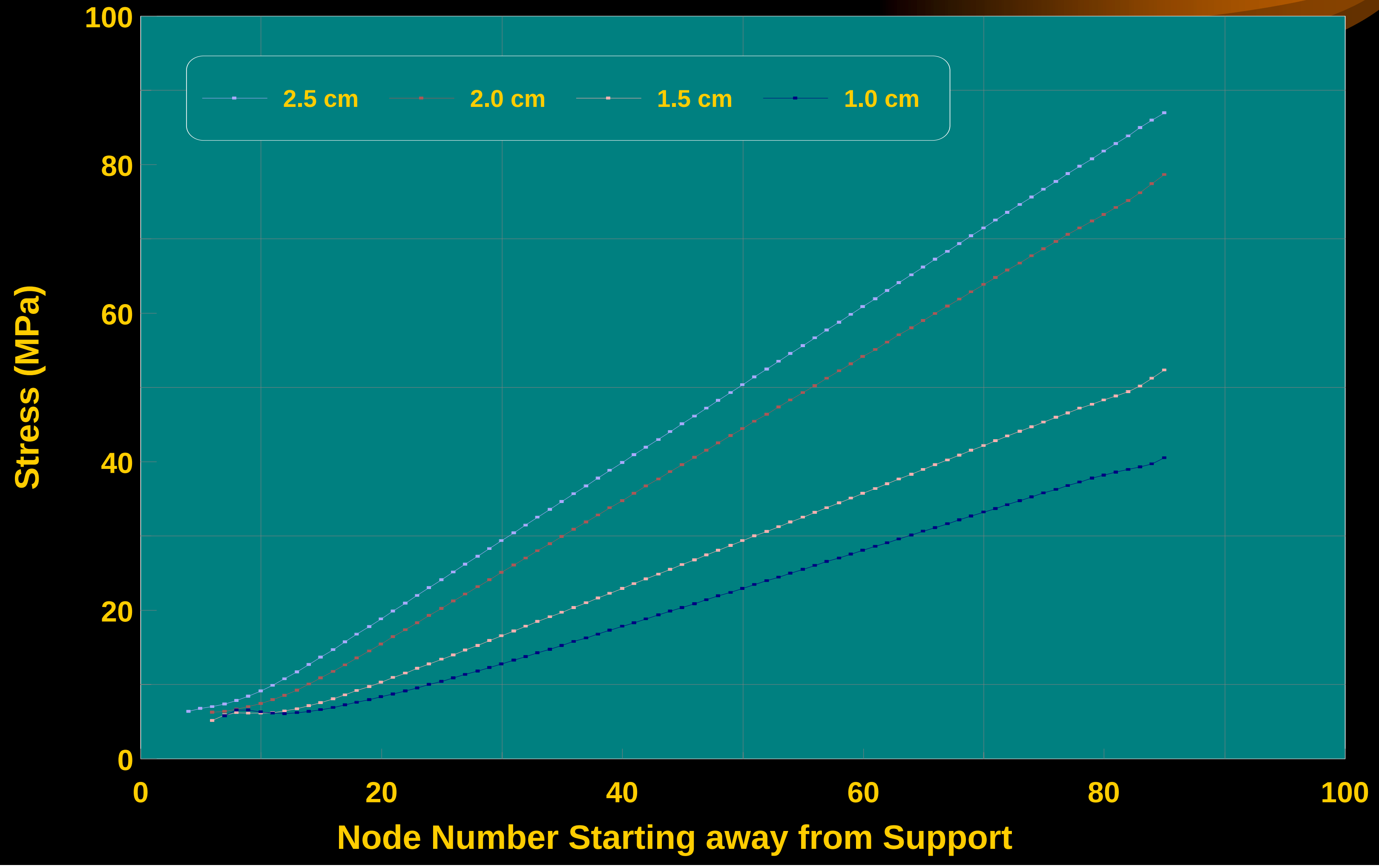

FEM-Predicted Maximum Strain of 12-Side Reduced-Size Composite Poles

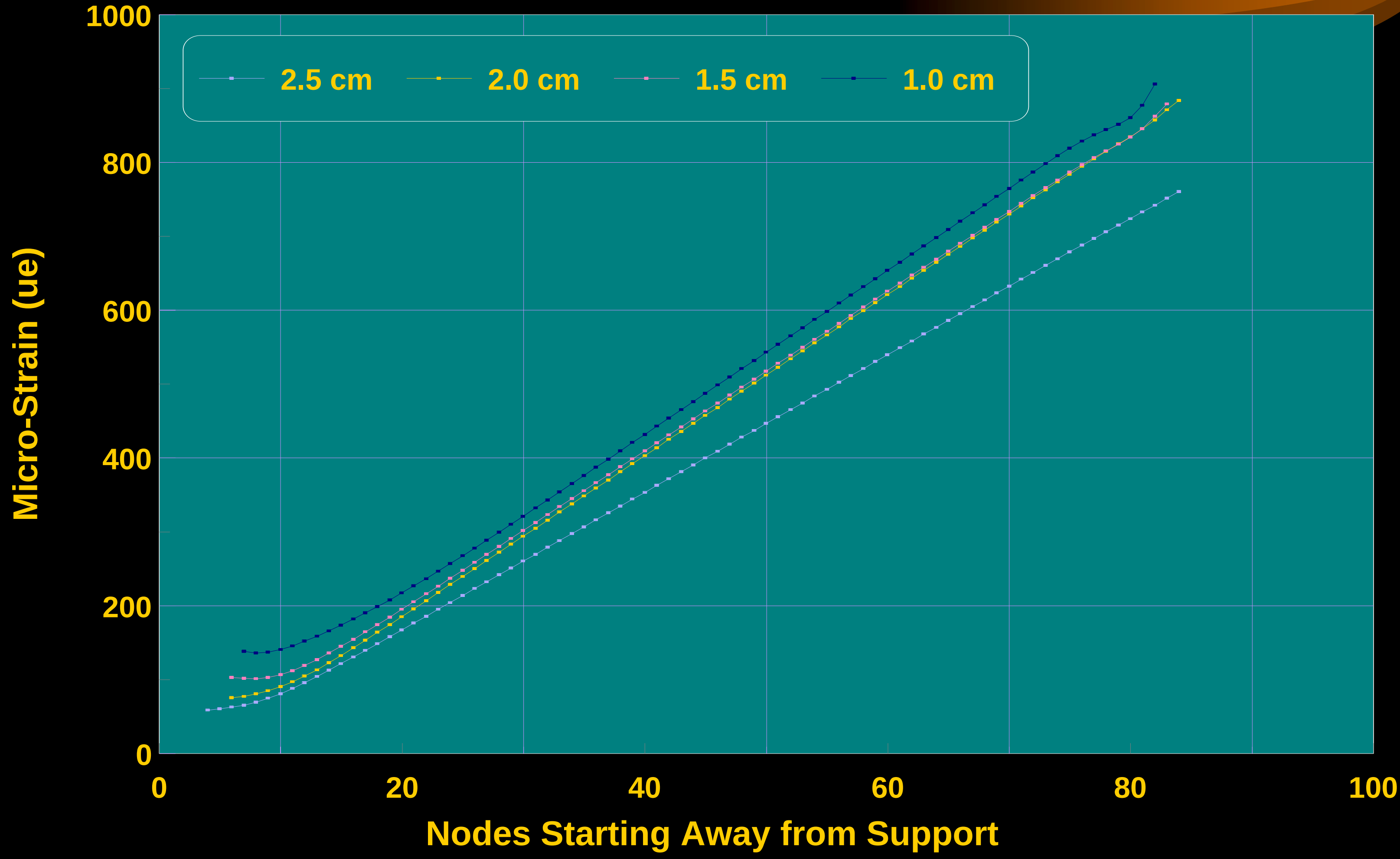

Deflection Comparison among Experimental, Theoretical, and FEM Values for 12-Side Reduced-Size Composite Poles

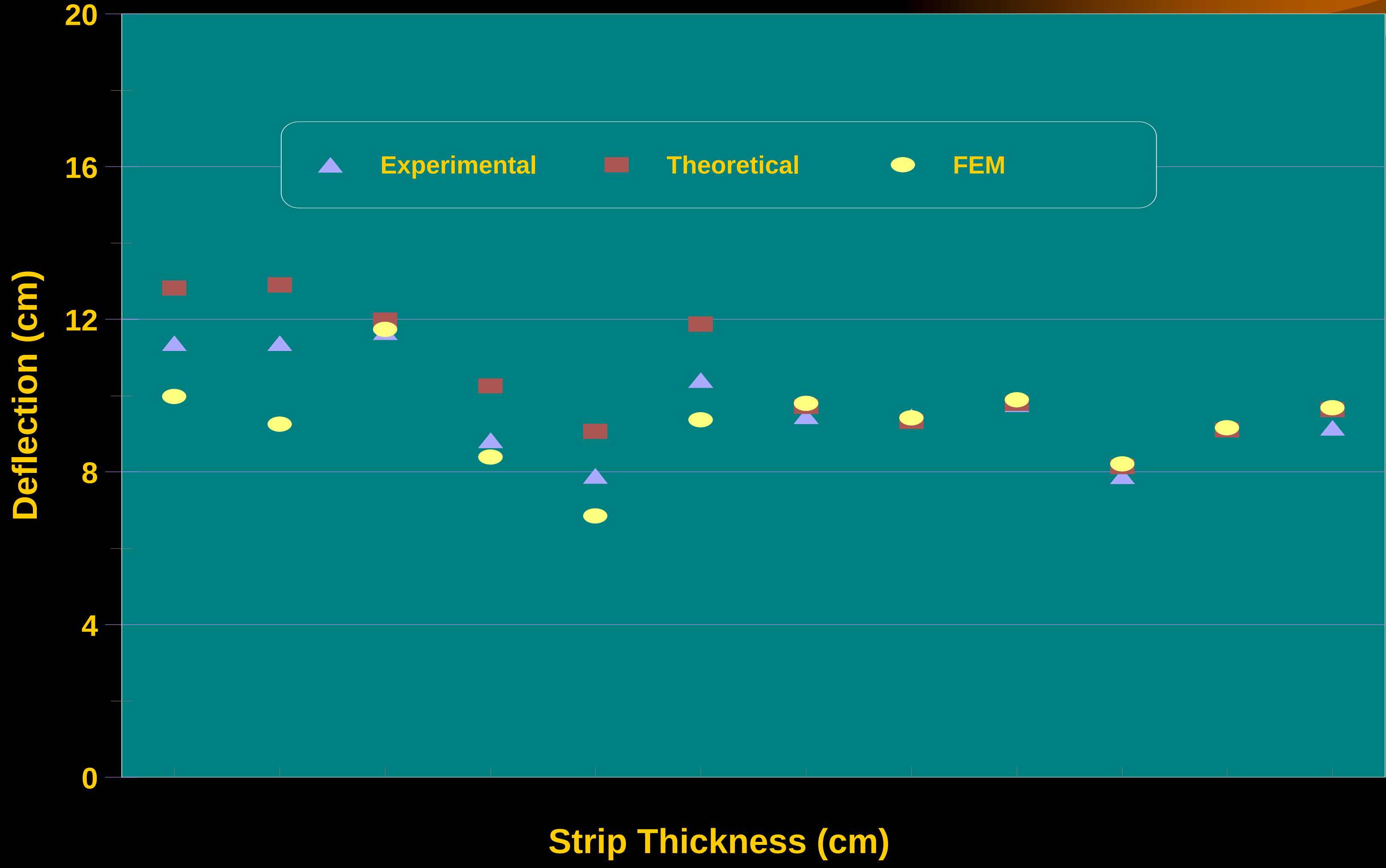

Conclusions

- The accuracy of the finite element results was first verified by the experiment data. The correlations are found to be good.

- The experimental values in deflection were 2 to 10 percent higher than the finite element ones. The maximum stress values show the same trend.

Conclusions (cont.)

- The finite element results were then compared to the results obtained from the theoretical study.

- The theoretical values were 1 to 5 percent higher than the finite elemental ones. Maximum stress values predicted by the finite element model were greater than those obtained from the theoretical study.

Conclusions (cont.)

- Maximum stress of composite poles in the cantilever test was in the parabolic areas on the top and bottom skins near the fixed end.

Deep Appreciations

- Dr. Shupe
- Dr. Hse
- Dr. Gopu
- Dr. DeHoop
- Ms. Pat
- Ms. Joann

Acknowledgement

- Mr. Xiaobo Li
- Mr. Yaojian Liu
- Mr. Dale
- Mr. Gerry

Good Memory of

- Dr. Choong

Thank You

?

? ?

?